

1 **Performance of bias correction schemes for CMORPH**
2 **rainfall estimates in the Zambezi River Basin**

3 **Webster Gumindoga¹², Tom H.M. Rientjes¹, Alemseged Tamiru Haile³, Hodson Makurira² and**
4 **Paolo Reggiani⁴**

5 *¹Faculty ITC, University of Twente, The Netherlands*

6 *²Civil Engineering Department, University of Zimbabwe, Zimbabwe*

7 *³International Water Management Institute (IWMI), Ethiopia*

8 *⁴University of Siegen, Germany*

9
10 *Email of corresponding author: w.gumindoga@utwente.nl*
11

12
13
14
15
16
17 Submission: 13 June 2019

18
19
20
21
22
23 *Email of corresponding author: w.gumindoga@utwente.nl*
24
25
26
27
28
29

1 Abstract

2 Satellite Rainfall Estimates (SRE) are prone to bias as they are indirect derivatives of the
3 visible, infrared, and/or microwave cloud properties, hence SREs need correction. We evaluate
4 the influence of elevation and distance from large scale open water bodies on bias for Climate
5 Prediction Center-MORPHing (CMORPH) rainfall estimates in the Zambezi Basin. The
6 effectiveness of five linear/non-linear and time-space variant/invariant bias correction schemes
7 was evaluated for daily rainfall estimates and climatic seasonality. Schemes used are: Spatio-
8 temporal Bias (STB), Elevation zone bias (EZ), Power transform (PT), Distribution
9 transformation (DT) and the Quantile mapping based on an empirical distribution (QME). We
10 used daily time series (1998-2013) from 60 gauge stations and CMORPH SREs for the
11 Zambezi Basin. To evaluate effectiveness of the bias correction techniques, spatial and
12 temporal cross-validation was applied based on 8 stations and on the 1998-1999 CMORPH
13 time series, respectively. For correction, STB and EZ schemes proved to be more effective in
14 removing bias. STB improved the correlation coefficient and Nash Sutcliffe efficiency by 50
15 % and 53 % respectively and reduced the root mean squared difference and relative bias by 25
16 % and 33 % respectively. Paired t-tests showed that there is no significant difference ($p < 0.05$)
17 in the daily means of CMORPH against gauge rainfall after bias correction. ANOVA post-hoc
18 tests revealed that the STB and EZ bias correction schemes are preferable. Bias is highest for
19 very light rainfall ($< 2.5 \text{ mm d}^{-1}$), for which most effective bias reduction is shown, in particular
20 for the wet season. Similar findings are shown through quantile-quantile (q-q) plots. The spatial
21 cross-validation approach revealed that the majority of the bias correction schemes removed
22 bias by $> 28 \%$. The temporal cross-validation approach showed effectiveness of the bias
23 correction schemes. Taylor diagrams show that station elevation has an influence on CMORPH
24 performance. Effects of distance $> 10 \text{ km}$ from large scale open water bodies are minimum
25 whereas the effect at shorter distances are indicated but not conclusive by lack of rain gauges.
26 Findings of this study show the importance of applying bias correction to SREs.

27

28 **Keywords:** *distance zone, elevation zone, satellite rainfall estimates, spatio-temporal bias,*
29 *Taylor diagram*

30

1

2 1. Introduction

3 Correction schemes for rainfall estimates are developed for climate models (Maraun, 2016;
4 Grillakis et al., 2017; Switanek et al., 2017), for radar approaches (Cecinati et al., 2017; Yoo et
5 al., 2014) and for satellite based, multi-sensor approaches (Najmaddin et al., 2017; Valdés-
6 Pineda et al., 2016). In this study focus is on satellite rainfall estimates (SREs) to improve
7 reliability in spatio-temporal rainfall representation.

8 Studies in satellite based rainfall estimation show that estimates are prone to systematic and
9 random errors (Gebregiorgis et al., 2012; Habib et al., 2014; Shrestha, 2011; Tesfagiorgis et al.,
10 2011; Vernimmen et al., 2012; Woody et al., 2014). Errors result primarily from the indirect
11 estimation of rainfall from visible (VIS), infrared (IR), and/or microwave (MW) based satellite
12 remote sensing of cloud properties (Pereira Filho et al., 2010; Romano et al., 2017). Systematic
13 errors in SREs commonly are referred to as bias, which is a measure that indicates the
14 accumulated difference between rain gauge observations and SREs. Bias in SREs is expressed
15 for rainfall depth (Habib et al., 2012b), rain rate (Haile et al., 2013) and frequency at which
16 rain rates occur (Khan et al., 2014). Bias may be negative or positive where negative bias
17 indicates underestimation whereas positive bias indicates overestimation (Liu, 2015; Moazami
18 et al., 2013).

19 Recent studies on the National Oceanic and Atmospheric Administration (NOAA) Climate
20 Prediction Center-MORPHing (CMORPH) (Wehbe et al., 2017; Jiang et al., 2016; Liu et al.,
21 2015; Haile et al., 2015) reveal that accuracy of this satellite rainfall product varies across
22 different regions (Gumindoga et al., 2019), but causes are not directly identifiable. As such
23 correction schemes serve to reduce systematic errors and to improve applicability of SREs.
24 Correction schemes rely on assumptions that adjust errors in space and/or time (Habib et al.,
25 2014). Some correction schemes consider correction only for spatial distributed patterns in
26 bias, commonly known as space variant/invariant. Approaches that correct for spatially
27 averaged bias have roots in radar rainfall estimation (Seo et al., 1999) but are unsuitable for
28 large scale basins ($> 5,000 \text{ km}^2$) where rainfall may substantially vary in space (Habib et al.,
29 2014). Studies by Tefsagiorgis et al. (2011) in Oklahoma (USA) and Müller and Thompson
30 (2013) in Nepal concluded that space variant correction schemes are more effective in reducing
31 CMORPH and TRMM bias than space invariant correction schemes. In a study conducted in
32 the Upper Blue Nile basin in Ethiopia, Bhatti et al. (2016) show that CMORPH bias correction
33 is most effective when bias factors are calculated for 7-day sequential windows.

34 Bias correction schemes based on regression techniques have reported distortion of frequency
35 of rainfall rates (Ines and Hansen, 2006; Marcos et al., 2018). Multiplicative shift procedures
36 tend to adjust SRE rainfall rates, but Ines and Hansen (2006) reported that they do not correct
37 systematic errors in rainfall frequency of climate models. Non-multiplicative bias correction
38 schemes preserve the timing of rainfall within a season (Fang et al., 2015; Hempel et al., 2013).

1 Studies that have applied non-linear bias correction schemes such as Power Function report
2 correction of extreme values (depth, rate and frequency) thus mitigating the underestimation
3 and overestimation of CMORPH rainfall (Vernimmen et al., 2012). The study by Tian (2010)
4 in the United States noted that the Bayesian (likelihood) analysis techniques are found to over-
5 adjust both light and heavy CMORPH rainfall.

6 Bias often exhibits a topographic and latitudinal dependency as, for instance, shown for
7 CMORPH product in the Nile Basin (Bitew et al., 2011; Habib et al., 2012a; Haile et al., 2013).
8 For Southern Africa, Thorne et al. (2001), Dinku et al. (2008) and Meyer et al. (2017) show that
9 bias in rainfall rate and frequency can be related to location, topography, local climate and
10 season. First studies in the Zambezi Basin (Southern Africa) on SREs show evidence that
11 necessitates correction of SREs. For example, Cohen Liechti (2012) show bias in CMORPH
12 SREs for daily rainfall and for accumulated rainfall at monthly scale. Matos et al. (2013),
13 Thiemig et al. (2012) and Toté et al. (2015) show that bias in rainfall depth at time intervals
14 ranging from daily to monthly varies across geographical domains in the Zambezi Basin and
15 may be as large as $\pm 50\%$. Besides elevation, there are indications that presence of Lake Tana
16 ($\approx 3050 \text{ km}^2$, Ethiopia) affects rainfall at short distances ($< 10\text{km}$) (Haile et al., 2009).

17 For less developed areas such as in the Zambezi Basin that is selected for this study, studies on
18 SREs are limited. This is despite the strategic importance of the basin in providing water to
19 over 30 million people (World Bank, 2010a). An exception is the study by Beyer et al. (2014)
20 on correction of the TRMM-3B42 product for agricultural purposes in the Upper Zambezi
21 Basin. Studies (Cohen Liechti et al., 2012; Meier et al., 2011) on use of SREs in the Zambezi
22 River Basin mainly focused on accuracy assessment of the SREs using standard statistical
23 indicators with little or no effort to perform bias correction despite the evidence of errors in
24 these products. The use of uncorrected SREs is reported for hydrological modelling in the Nile
25 Basin (Bitew and Gebremichael, 2011) and Zambezi Basin (Cohen Liechti et al., 2012),
26 respectively, and for drought monitoring in Mozambique (Toté et al., 2015). The poor
27 performance of SREs in above studies urges for bias correction to result in more accurate
28 rainfall representation. The selection of CMORPH satellite rainfall for this study is based on
29 successful applications of bias corrected CMORPH estimates in African basins for
30 hydrological modelling (Habib et al., 2014) and flood predictions in West Africa (Thiemig et
31 al., 2013). In first publications on CMORPH, Joyce et al. (2004) describe CMORPH as a
32 gridded precipitation product that estimates rainfall with information derived from IR data and
33 MW data. CMORPH combines the retrieval accuracy of passive MW estimates with IR
34 measurements which are available at high temporal resolution but with low accuracy. The
35 important distinction between CMORPH and other merging methods is that the IR data are not
36 used for rainfall estimation but used only to propagate rainfall features that have been derived
37 from microwave data. The flexible ‘morphing’ technique is applied to modify the shape and
38 rate of rainfall patterns. CMORPH is operational since 2002 for which data is available at the
39 CPC of the National Centers for Environmental Prediction (NCEP) (after

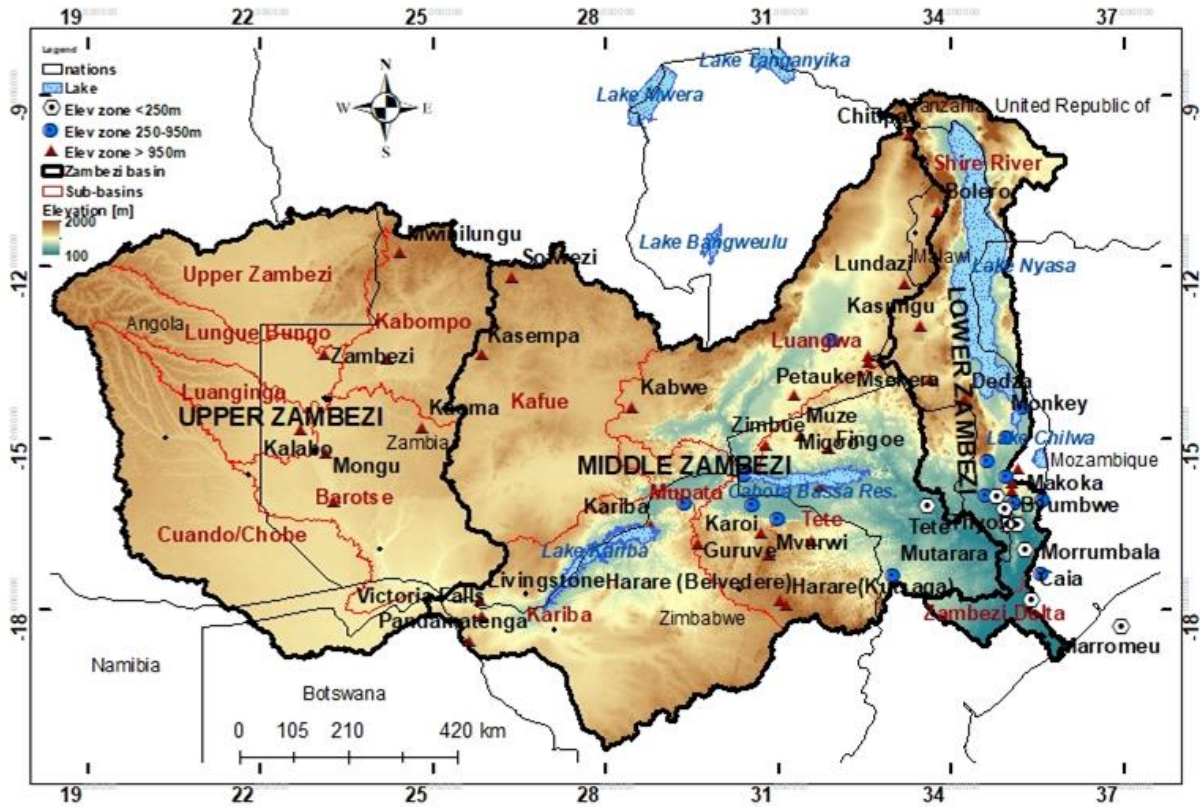
1 <http://www.ncep.noaa.gov/>). Recent publications on CMORPH in African basins exist (Wehbe
2 et al., 2017; Koutsouris et al., 2016; Jiang et al., 2016; Haile et al., 2015). However, studies on
3 bias correction of CMORPH in the semi-arid Zambezi Basin are limited.

4 In this study we use daily CMORPH and rain gauge data for Upper, Middle, and Lower
5 Zambezi basins to (1) evaluate if performance of CMORPH rainfall is affected by elevation
6 and distance from large scale open water bodies (2) evaluate the effectiveness of linear/non-
7 linear and time-space variant/invariant bias correction schemes and (3) assess the performance
8 of bias correction schemes to represent different rainfall rates and climate seasonality. Analysis
9 serve to improve reliability of SREs applications in water resource applications in the Zambezi
10 basin such as for rainfall-runoff modeling.

11 **1. Study area**

12 The Zambezi River is the fourth-longest river (~2,574 km) in Africa with basin area of
13 ~1,390,000 km² (~4 % of the African continent). The river drains into the Indian Ocean and
14 has mean annual discharge of 4,134 m³/s (World Bank, 2010a). The river has its source in
15 Zambia with basin boundaries in Angola, Namibia Botswana, Zambia, Zimbabwe and
16 Mozambique (Figure 1). The basin is characterized by considerable differences in elevation
17 and topography, distinct climatic seasons and presence of large-scale open water bodies and,
18 as such, makes the basin well suited for this study. The basin is divided into three sub-basins
19 i.e., the Lower Zambezi comprising the Tete, Lake Malawi/Shire, and Zambezi Delta basins,
20 the Middle Zambezi comprising the Kariba, Mupata, Kafue, and Luangwa basins, and the
21 Upper Zambezi comprising the Kabompo, Lungwebungo, Luanginga, Barotse, and
22 Cuando/Chobe basins (Beilfuss, 2012).

23 The elevation of the Zambezi basin ranges from < 200 m (for some parts of Mozambique) to
24 >1500 m above sea level (for some parts of Zambia). Large scale open water bodies in and
25 around the basin are Kariba, Cabora Bassa, Bangweulu, Chilwa and Nyasa. The Indian Ocean
26 lies to the east of Mozambique. Typical landcover types are woodland, grassland, water
27 surfaces and cropland (Beilfuss et al., 2000). The basin lies in the tropics between 10 and 20
28 degrees South, encompassing humid, semi-arid and arid regions dominated by seasonal rainfall
29 patterns associated with the Inter-Tropical Convergence Zone (ITCZ), a convective front
30 oscillating along the equator (Cohen Liechti et al., 2012). The movement of the ITCZ in
31 Southern hemisphere results in the peak rainy season that occurs during the summer (October
32 to April) and the dry winter months (May-Sept) is a result of the shifting back of ITCZ towards
33 the equator (Schlosser and Strzepek, 2015). The weather system in South Eastern parts such as
34 Mozambique is dominated by Antarctic Polar Fronts (APF) and Tropical Temperate Troughs
35 (TTTs) occurrence which is positively related to La Niña and Southern Hemisphere planetary
36 waves, while El Niño-Southern Oscillation (ENSO) appears to play a significant role in causing
37 dry conditions in the basin (Beilfuss, 2012).



1

2 Figure 1: Zambezi River Basin from Africa with sub basins, major lakes, elevation, and locations and names of the 60 rain
 3 gauging stations (in each respective elevation zone) used in this study.

4 The basin is characterized by high annual rainfall ($> 1\,400\text{ mm yr}^{-1}$) in the northern and north-
 5 eastern areas and by low annual rainfall ($< 500\text{ mm yr}^{-1}$) in the southern and western parts
 6 (World Bank, 2010b). Due to this rainfall distribution, northern tributaries in the Upper
 7 Zambezi sub-basin contribute 60 % of the mean annual discharge (Tumbare, 2000). The river
 8 and its tributaries are subject to seasonal floods and droughts that have devastating effects on
 9 the people and economies of the region, especially the poorest members of the population
 10 (Tumbare, 2005). It is not uncommon to experience both floods and droughts within the same
 11 hydrological year.

12 **3. Materials and Methodology**

13 **3.1. Rainfall data**

14 **3.1.1. CMORPH**

15 For this study, time series of CMORPH rainfall images (1998-2013) at $8\text{ km} \times 8\text{ km}$, 30-minute
 16 resolution were selected and downloaded from the NOAA repository
 17 (ftp://ftp.cpc.ncep.noaa.gov/prep/CMORPH_V1.0/CRT/8km.30m/). Images are downloaded
 18 by means of the GeoNETCAST ISOD toolbox of ILWIS GIS software
 19 (<http://52north.org/downloads/>). Half hourly estimates were aggregated to daily totals to match
 20 the observation interval of gauge based daily rainfall.

1 3.1.2. *Rain gauge network*

2 Time series of daily rainfall from 60 stations were obtained from meteorological departments
3 in Botswana, Malawi, Mozambique, Zambia and Zimbabwe for stations that cover the study
4 area. All the stations are standard type rain gauges with a measuring cylinder whose unit of
5 measurement is millimetres (mm).

6 Some stations are affected by data gaps but the available time series are of sufficiently long
7 duration (see Appendix 1) to serve the objectives of this study. Stations are irregularly
8 distributed across the vast basin and are located at elevation between 3 m to 1575 m (Figure
9 1). The minimum, maximum and average distance between the rain gauges is 3.5 km (Zumbo
10 in Mozambique-Kanyemba in Zimbabwe), 1570 km (Mwinilunga in Zambia-Marromeu in
11 Mozambique) and 565 km respectively. Distances to large scale open water bodies range
12 between 5 km and 615 km. This allows us to evaluate if elevation and distance to large scale
13 open water bodies affect CMORPH performance.

14 3.1.1. *Comparison of CMORPH and gauge rainfall*

15 In this study, we compare gauge rainfall at point scale to CMORPH satellite derived rainfall
16 estimates at pixel scale (point-to-pixel). Comparison is at a daily time interval covering the
17 period 1998-2013, following Cohen Liechti et al. (2012), Dinku et al. (2008), Haile et al.
18 (2014), Hughes (2006), Tsidu (2012) and Worqlul et al. (2014) who report on point-to-pixel
19 comparisons in African basins. We apply point-to-pixel comparison to rule out any aspect of
20 interpolation error as a consequence of the low-density network with unevenly distributed
21 stations. We refer to Heidinger et al. (2012), Li and Heap (2011), Tobin and Bennett (2010) and
22 Yin et al. (2008) who report that interpolation introduces unreliability and uncertainty to pixel-
23 based rainfall estimates. Also, Worqlul et al. (2014) describe that for pixel-to-pixel comparison,
24 there is demand for a well distributed rain gauge network that would not hamper accurate
25 interpolation.

26 3.2. **Elevation and distance from large scale open water bodies**

27 Habib et al. (2012a) and Haile et al. (2009) for the Nile Basin reveal that elevation affect
28 performance of SREs. Findings in the latter two studies signal that performance possibly also
29 may be affected by presence of Lake Tana. To assess both influences, we classified the Zambezi
30 Basin into 3 elevation zones for which the hierarchical cluster ‘within-groups linkage’ method
31 in the Statistical Product and Service Solutions (SPSS) software was used (Table 1). Based on
32 Euclidian distance to large-scale open water bodies, 4 arbitrary distance zones are defined to
33 group stations (Table 1). A detailed description on the individual stations, their elevation and
34 distance to large-scale open water bodies is provided in Appendix 1. The Advanced Spaceborne
35 Thermal Emission and Reflection Radiometer (ASTER) based DEM of 30 m resolution
36 obtained from <http://gdem.ersdac.jspacesystems.or.jp/>, is used to represent elevation across the
37 Zambezi Basin. The Euclidian distance of each rain gauge location to large-scale open water

1 bodies is defined in a GIS environment through the distance calculation algorithm. Large-scale
 2 open water bodies are defined as perennial open water bodies with surface area $> 700 \text{ km}^2$. The
 3 threshold is defined based on knowledge of the water bodies in the Zambezi basin study area
 4 and the detailed fieldwork the authors have conducted over the years in various other study
 5 areas in Africa (such as Lake Tana in Ethiopia and Lake Naivasha in Kenya). The relationship
 6 between lake surface area and CMORPH bias on 300 water bodies in the study area shows that
 7 at a threshold $> 700 \text{ km}^2$, a signal is induced to warrant the removal from the analysis of all
 8 water bodies with surface area $< 700 \text{ km}^2$.

9 Table 1: Elevation and distance from large scale open water bodies

Zone ID	Elevation (m)	No. of stations	Mean elevation of stations (m)
Zone 1	< 250	8	90
Zone 2	250-950	21	510
Zone 3	> 950	31	1140

Zone ID	Distance (km)	No. of stations	Mean distance to large-scale open water bodies (km)
Zone 1	< 10 km	4	5
Zone 2	10 - 50	10	35
Zone 3	50 - 100	18	80
Zone 4	> 100	28	275

10

11 3.3. Bias correction schemes

12 Bias correction schemes evaluated in this study are the Spatio-temporal bias (STB), Elevation
 13 zone bias (EZ), Power transform (PT), Distribution transformation (DT), and the Quantile
 14 mapping based on an empirical distribution (QME), this by our aim to correct for bias while
 15 daily rainfall variability is preserved. The five schemes are chosen based on merits documented
 16 in literature (Bhatti et al., 2016; Habib et al., 2014; Teutschbein and Seibert, 2013; Themeßl et
 17 al., 2012; Vernimmen et al., 2012). We note that findings on the performance of selected bias
 18 correction schemes in literature do not allow for generalization but findings only apply to the
 19 respective study domains (Wehbe et al., 2017; Jiang et al., 2016; Liu et al., 2015; Haile et al.,
 20 2015).

21 In the procedure to define a time window for bias correction we follow Habib et al. (2014) and
 22 Bhatti et al. (2016) who in the Lake Tana Basin (Ethiopia) carried out a sensitivity analysis on
 23 moving time windows and on sequential time windows. Window lengths between 3 and 31
 24 days are tested. Findings indicated that a 7-day sequential time window for bias factors is most
 25 appropriate but only when a minimum of five rainy days were recorded within the 7-day
 26 window with a minimum rainfall accumulation depth of 5 mm d^{-1} , otherwise no bias is
 27 estimated (i.e. a value of 1 applies as bias correction factor). Preliminary tests in this study on
 28 5 and 7-day moving and sequential windows on 20 individual stations distributed over the three

1 elevation zones indicates that the 7-day sequential approach is well applicable in the Zambezi
2 Basin. As such, the approach was selected.

3 The bias correction factors are calculated using only rain days (rainfall ≥ 1 mm d⁻¹). Otherwise
4 in cases where both the gauge and satellite have zero values (Rain gauge (G)=0 and CMORPH
5 (S) =0), correction is not applied and the SRE value remains 0 mm d⁻¹.

6 Following Bhatti et al. (2016), we spatially interpolate the bias correction factors of the rain
7 gauges so that SREs at all pixels can be corrected. For interpolation, the Universal Kriging was
8 applied. Thus, to systematically correct all CMORPH estimates, station based bias factors for
9 each time window are spatially interpolated to arrive at spatial coverage across the study area
10 and to allow for comparison with other approaches.

11 3.3.1. *Spatio-temporal bias correction (STB)*

12 This linear bias correction scheme has its origin in the correction of radar-based precipitation
13 estimates (Tefagiorgis et al., 2011) and downscaled precipitation products from climate
14 models. The CMORPH daily rainfall estimates (S) are multiplied by the bias correction factor
15 for the respective sequential time window for individual stations resulting in corrected
16 CMORPH estimates (STB) in a temporally and spatially coherent manner (Equation [1]).

17

$$18 \quad STB = S \frac{\sum_{t=d}^{t=d-l} G(i,t)}{\sum_{t=d}^{t=d-l} S(i,t)} \quad [1]$$

19 Where:

20 G = gauged rainfall (mm d⁻¹)

21 i = gauge number

22 d = day number

23 t = julian day number

24 l = length of a time window for bias correction

25

26 The advantages of this bias correction scheme are that it is straightforward and easy to
27 implement due to its simplicity and modest data requirements. However, just like any
28 multiplicative shift procedures of bias correction, STB has challenges in correcting systematic
29 errors in rainfall frequency particularly the wet-day frequencies (Lenderink et al., 2007;
30 Teutschbein and Seibert, 2013).

31 3.3.2. *Elevation zone bias correction (EZ)*

32 This bias scheme is proposed in this study and aims at correcting satellite rainfall for elevation
33 influences. This method groups rain gauge stations into 3 elevation zones based on station
34 elevation. The grouping in this study is based on the hierarchical clustering technique, expert

1 knowledge about the study area but also guided by relevant past studies in the basin (e.g. World
 2 Bank, 2010b; Beilfuss, 2012). Each zone has the same bias correction factor but differs across
 3 the three zones. In the time domain bias factors vary following the 7-day sequential window
 4 approach. The corrected CMORPH estimates (EZ) at daily time interval are obtained by
 5 multiplying the uncorrected CMORPH daily rainfall estimates (S) by the daily bias correction
 6 factor of each elevation zone.

$$EZ = S \frac{\sum_{t=d-l}^{t=d-1} \sum_{i=1}^{i=n} G(i, t)}{\sum_{t=d-l}^{t=d-1} \sum_{i=1}^{i=n} S(i, t)} \quad [2]$$

9
 10 The merit of this bias correction scheme is that the effects of elevation on rainfall depth are
 11 accounted for. SREs often have difficulties in capturing rainfall events due to orographic effects
 12 and thus require elevation-based correction.

13 14 3.3.3. Power transform (PT)

15 The non-linear PT bias correction scheme has its origin in studies of climate change impact
 16 (Lafon et al., 2013). Vernimmen et al. (2012) show that the scheme could be applied to correct
 17 satellite rainfall estimates for use in hydrological modelling and drought monitoring. The PT
 18 method uses an exponential form to adjust the standard deviation of rainfall series. The daily
 19 bias corrected CMORPH rainfall (PT) for a pixel that overlays a station is obtained using
 20 equation:

$$PT = aG(i, t)^b \quad [3]$$

21
 22 *Where:*

23 G = gauged rainfall (mm d⁻¹)

24 a = prefactor such that the mean of the transformed CMORPH values is equal to the
 25 mean of rain gauge rainfall

26 b = factor calculated such that for each rain gauge the coefficient of variation (CV) of
 27 CMORPH matches the gauge based counter parts

28 i = gauge number

29 t = day number

30 Optimized values for a and b are obtained through the generalized reduced gradient algorithm
 31 (Fylstra et al., 1998). Values for a and b vary for the 7-day sequential window since correction
 32 is at daily time base. In the case of utilizing the PT method in a certain area (or for a certain
 33 period), the bias correction factor is spatially interpolated to result in comparable estimates with
 34 other bias correction schemes. The advantage of the bias scheme is that it adjusts extreme
 35 precipitation values in CMORPH estimates (Vernimmen et al., 2012). PT has reported

1 limitations in correcting wet-day frequencies and intensities (Leander et al., 2008; Teutschbein
2 and Seibert, 2013).

3 4 3.3.4. *Distribution transformation (DT)*

5 DT is an additive bias correction approach which has its origin in statistical downscaling of
6 climate model data (Bouwer et al., 2004). The method transforms a statistical distribution
7 function of daily CMORPH rainfall estimates to match the distribution by gauged rainfall. The
8 procedure to match the CMORPH distribution function to gauge rainfall based counter parts is
9 described in equations [4-8]. The principle to matching is that the difference in the mean value
10 and differences in the variance are corrected for, in the 7-day sequential window. First, the bias
11 correction factor for the mean is determined by equation [4]:

$$12 \quad DT_u = \frac{G_u}{S_u} \quad [4]$$

13 G_u and S_u are mean values of 7-day gauge and CMORPH rainfall estimates.

14
15 Secondly, the correction factor for the variance ($DT\tau$) is determined by the quotient of the 7-
16 day standard deviations, $G\tau$ and $S\tau$, for gauge and CMORPH respectively.

$$18 \quad DT\tau = \frac{G\tau}{S\tau} \quad [5]$$

19 Once the correction factors which vary within a 7-day time sequential window are established,
20 they are then applied to correct all daily CMORPH estimates (S) through equation [6] to obtain
21 corrected CMORPH rainfall estimate (DT). The parameters DTu and are developed within a 7-
22 day sequential window but correction is at daily time intervals.

$$24 \quad DT = (S(i, t) - S_u)DT\tau + DTu * S\tau \quad [6]$$

23
26 Uncorrected CMORPH daily values are returned if [6] results in negative values. The merit of
27 this bias correction scheme is that it corrects wet-day frequencies and intensities. The
28 disadvantage of this bias correction scheme is that adding the gauge based mean deviation to
29 the satellite data destroys the physical consistency of the data. In addition, the method might
30 result in the generation of too few rain days in the wet season, and sometimes the mean of daily
31 intensities might be unrealistically corrected (Johnson and Sharma, 2011; Teutschbein and
32 Seibert, 2013).

33 34 3.3.5. *Quantile mapping based on an empirical distribution (QME)*

1 This is a quantile based empirical-statistical error correction method with its origin in empirical
 2 transformation and bias correction of regional climate model-simulated precipitation (Themeßl
 3 et al., 2012). The method corrects CMORPH precipitation based on empirical cumulative
 4 distribution functions (*ecdfs*) which are established for each 7-day time window and for each
 5 station. The bias corrected rainfall (*QME*) using quantile mapping are expressed in terms of the
 6 empirical cumulative distribution function (*ecdf*) and its inverse ($ecdf^{-1}$). Parameters apply to a
 7 7-day sequential window but correction is then at daily time interval with bias spatially
 8 averaged for the entire domain to allow for comparison with other approaches

$$9 \quad QME = ecdf_{obs}^{-1}(ecdf_{raw}(S(i, t))) \quad [7]$$

11 Where:

12 $ecdf_{obs}$ = empirical cumulative distribution function for the gauge-based observation

13 $ecdf_{raw}$ = empirical cumulative distribution function for the uncorrected CMORPH

14 The advantage of this bias scheme is that it corrects quantiles and preserves the extreme
 15 precipitation values (Themeßl et al., 2012). However, it also has its limitation due to the
 16 assumption that both the observed and satellite rainfall follow the same proposed distribution,
 17 which may introduce potential new biases.

18 3.4. Rainfall rates and seasons

19 To assess the performance of SREs for different classes of daily rainfall rates five classes are
 20 defined which indicate: very light (< 2.5 mm d⁻¹), light (2.5-5.0 mm d⁻¹), moderate (5.0-10.0
 21 mm d⁻¹), heavy (10.0-20.0 mm d⁻¹) and very heavy rainfall (> 20.0 mm d⁻¹).

22 Furthermore, gauged rainfall was divided into wet and dry seasonal periods to assess the
 23 influence of seasonality on performance of bias correction schemes. The wet season in the
 24 Zambezi Basin spans from October-March whereas the dry season spans from April-
 25 September.

26 3.5. Evaluation of CMORPH estimates

27 Corrected and uncorrected CMORPH satellite rainfall estimates are evaluated with reference
 28 to rain gauge rainfall using statistics that measure systematic differences (i.e. percentage bias
 29 and Mean Absolute Error (MAE)), measures of association (e.g. correlation coefficient and
 30 Nash Sutcliffe Efficiency (NSE) and random differences (e.g. standard deviation of differences
 31 and coefficient of variation) (Haile et al., 2013). Bias is a measure of how the satellite rainfall
 32 estimate deviates from the rain gauge rainfall, and the result is normalised by the summation
 33 of the gauge values. A positive value indicates overestimation whereas a negative value
 34 indicates underestimation. The correlation coefficient (ranging between +1 and -1) represents
 35 the linear dependence of gauge and CMORPH data. MAE is the arithmetic average of the

1 absolute values of the differences between the daily gauge and CMORPH satellite rainfall
 2 estimates. The MAE is zero if the rainfall estimates are perfect and increases as discrepancies
 3 between the gauge and satellite become larger. NSE indicates how well the satellite rainfall
 4 matches the rain gauge observation and it ranges between $-\infty$ and 1, with $NSE = 1$ meaning a
 5 perfect fit (Nash and Sutcliffe, 1970).

6 Equations [8-11] apply.

$$7 \quad bias (\%) = \frac{\sum(S-G)}{\sum G} * 100 \quad [8]$$

$$8 \quad R = \frac{\sum(G-\bar{G})(S-\bar{S})}{\sqrt{\sum(G-\bar{G})^2}\sqrt{\sum(S-\bar{S})^2}} \quad [9]$$

$$9 \quad MAE = \frac{1}{n} \sum |S - G| \quad [10]$$

$$10 \quad NSE = \frac{\sum(G-S)^2}{\sum(G-\bar{G})^2} \quad [11]$$

11 Where:

12 S = satellite rainfall estimates (mm d⁻¹)

13 \bar{S} = mean of the satellite rainfall estimates (mm d⁻¹)

14 G = rainfall by a rain gauge (mm d⁻¹)

15 \bar{G} = mean values of rainfall recorded by a rain gauge (mm d⁻¹)

16 n = number of observations

17 3.6. Test for differences of mean

18 To detect significant differences between gauge and satellite rainfall (corrected and
 19 uncorrected) and differences amongst the five bias correction methods described in Section
 20 3.3, we apply paired t-test and analysis of variance (ANOVA) tests.

21 3.6.1. Paired t-tests

22 A paired t-test was used to test whether there is a significant difference between rain gauge,
 23 uncorrected and bias corrected CMORPH satellite rainfall for the 52 rain gauges. Results are
 24 summarized for the Upper, Lower and Middle Zambezi. The paired t-test compares the mean
 25 difference of the values to zero. It depends on the mean difference, the variability of the
 26 differences and the number of data. The null hypothesis (H_0) is that there is no difference in
 27 mean gauge and satellite daily rainfall (uncorrected and bias corrected). If the p-value is less
 28 than or equal 0.05 (5%), the result is deemed statistically significant, i.e., there is a significant
 29 relationship between the gauge and satellite rainfall (Wilks, 2006; Field, 2009).

30 3.6.2. Analysis of Variance (ANOVA) test

1 The ANOVA-test aims to test whether there is a significant difference amongst the 5 bias
2 correction techniques. The Null hypothesis (H_0) is that there are no differences amongst the
3 five bias correction schemes. We further determined which schemes differ significantly using
4 3 post-hoc tests, namely: Tukey HSD, Scheffe and the Bonferroni (Brown, 2005; Kucuk et al.,
5 2018). Results are summarized for the Upper, Lower and Middle Zambezi.

6 3.7. Taylor diagram

7 We apply a Taylor diagram to evaluate differences in data sets generated by respective bias
8 correction schemes by providing a summary of how well bias correction results match gauge
9 rainfall in terms of pattern, variability and magnitude of the variability. Visual comparison of
10 SRE performance is done by analysing how well patterns match each other in terms of the
11 Pearson's product-moment correlation coefficient (R), root mean square difference (E), and the
12 ratio of variances on a 2-D plot (Lo Conti et al., 2014; Taylor, 2001). The reason that each point
13 in the two-dimensional space of the Taylor diagram can represent the above three different
14 statistics simultaneously is that the centered pattern of root mean square difference (E^i), and
15 the ratio of variances are related by the following:

$$16 \quad E^i = \sqrt{\sigma_f^2 + \sigma_r^2 - 2\sigma_f\sigma_r R} \quad [12]$$

17

18 Where:

19 σ_f and σ_r = standard deviation of CMORPH and rain gauge rainfall, respectively.

20

21 Development and applications of Taylor diagrams have roots in climate change studies
22 (Smiatek et al., 2016; Taylor, 2001) but also has frequent applications in environmental model
23 evaluation studies (Cuvelier et al., 2007; Dennis et al., 2010; Srivastava et al., 2015). Bhatti et
24 al. (2016) propose the use of Taylor Diagrams for assessing effectiveness of SREs bias
25 correction schemes. The most effective bias correction schemes will have data that lie near a
26 point marked 'reference' on the x-axis, relatively high correlation coefficient and low root mean
27 square difference. Bias correction schemes matching gauged based standard deviation have
28 patterns that have the right amplitude.

29 3.8. Quantile-quantile (q-q) plots

30 A q-q plot is used to check if two datasets (in this case gauge vs CMORPH rainfall) can fit the
31 same distribution (Wilks, 2006). A q-q plot is a plot of the quantiles of the first data set against
32 the quantiles of the second data set. A 45-degree reference line is also plotted. If the satellite
33 rainfall (corrected and uncorrected) has the same distribution as the rain gauge, the points
34 should fall approximately along this reference line. The greater the departure from this
35 reference line, the greater the evidence for the conclusion that the bias correction scheme is
36 less effective (NIST/SEMATECH, 2001).

1 The main advantage of the q-q plot is that many distributional aspects can be simultaneously
2 tested. For example, changes in symmetry, and the presence of outliers can all be detected from
3 this plot.

4 3.9. Cross validation of bias correction

5 3.9.1. Spatial cross-validation

6 The spatial cross-validation procedure (hold-out sample) applied in this study, involves the
7 withdrawal of 8 in-situ stations from the sample of 60 when generating bias corrected SREs
8 for all pixels across the study area. Corrected SREs are then compared to the rain gauge rainfall
9 of the withdrawn stations to evaluate closeness of match. From the sample of 8 we selected 2
10 stations in the < 250 m elevation zone, 3 stations in the 250-950 m zone and 3 stations in > 950
11 m elevation zone. Stations selected have elevation close to the average elevation zone value
12 and are centred in an elevation zone. This left us with 52 stations for applying the bias
13 correction methods and spatial interpolation. As performance indicators to evaluate results of
14 cross-validation, we use the percentage bias, MAE, Correlation Coefficient and the estimated
15 ratio which is obtained by dividing CMORPH rainfall totals and gauge-based rainfall totals for
16 the 1999-2013 period.

17 3.9.2. Temporal cross-validation

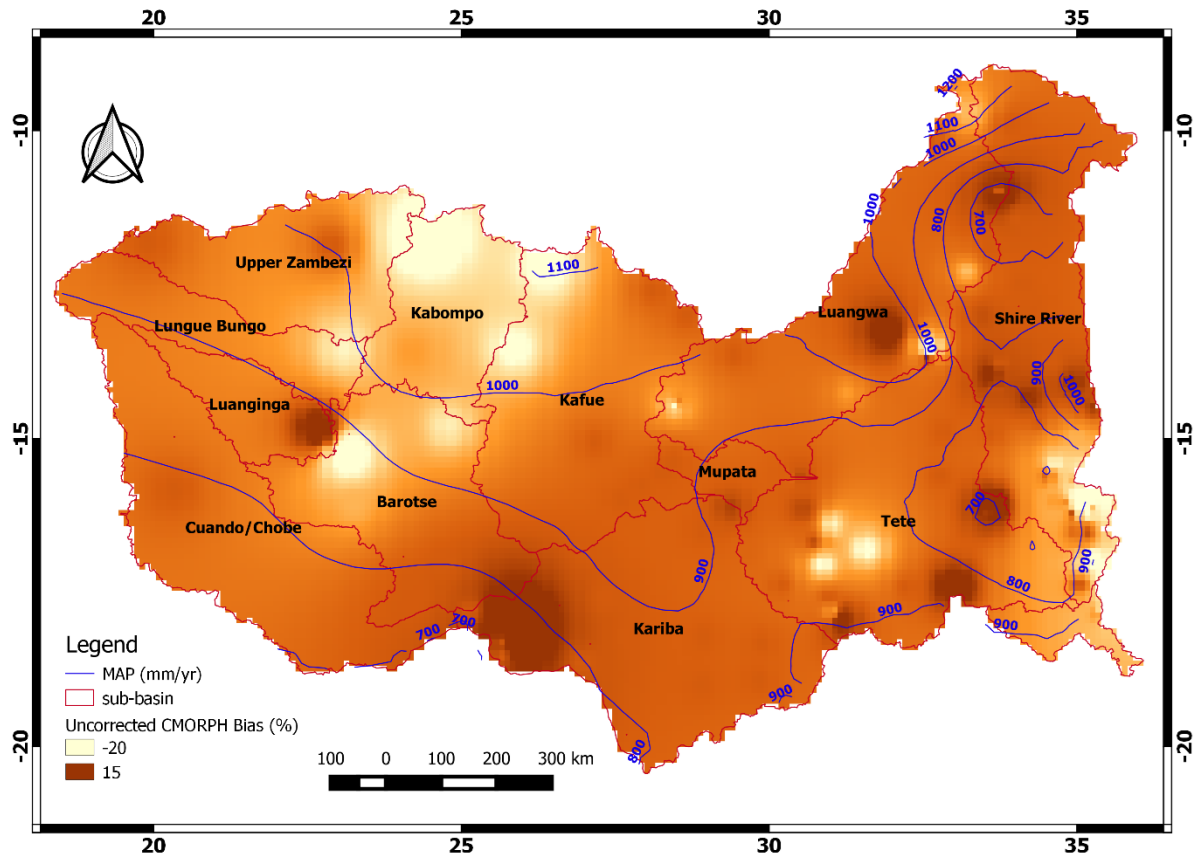
18 For evaluation of SREs in the time domain we followed Gutjahr and Heinemann (2013) to omit
19 rainfall (both from gauge and satellite) for the 1998-1999 hydrological year to remain with 14
20 years for bias correction of SREs. Bias corrected estimates for the 14 years are then evaluated
21 against estimates for 1998-1999 period that served as reference. For evaluation we use the
22 percentage bias, MAE, correlation coefficient and the estimated ratio, that all are averaged for
23 the Upper, Middle and Lower Zambezi but also for the wet and dry seasons.

24 4. Results and Discussion

25 4.1. Performance of uncorrected CMORPH rainfall

26 The spatially interpolated values of bias (%) across the Zambezi Basin are shown in Figure 2.
27 Areas in the central and western part of the basin have bias relatively close to zero suggesting
28 good performance of the uncorrected CMORPH product. However, relatively large negative
29 bias values (-20 %) are shown in the Upper Zambezi's high elevated areas such as Kabompo
30 and northern Barotse Basin, in the south-eastern part of the basin such as Shire River Basin and
31 in in the Lower Zambezi's downstream areas where the Zambezi River enters the Indian Ocean.
32 CMORPH overestimates rainfall locally in Kariba, Luanginga, and Luangwa basins by positive
33 bias values. As such CMORPH estimates do not consistently provide results that match rain
34 gauge observations. Since CMORPH estimates have pronounced error ($-10 > \text{bias} (\%) > 10$),
35 bias needs to be removed before the product can be applied for hydrological analysis and in
36 water resources applications. Figure 2 also shows contours for rain gauge mean annual

- 1 precipitation (MAP) in the Zambezi Basin with higher values in the northern parts of the basin
- 2 (Kabompo and Luangwa) compared to localised estimates of MAP such as in Shire River and
- 3 Kariba sub-basins.

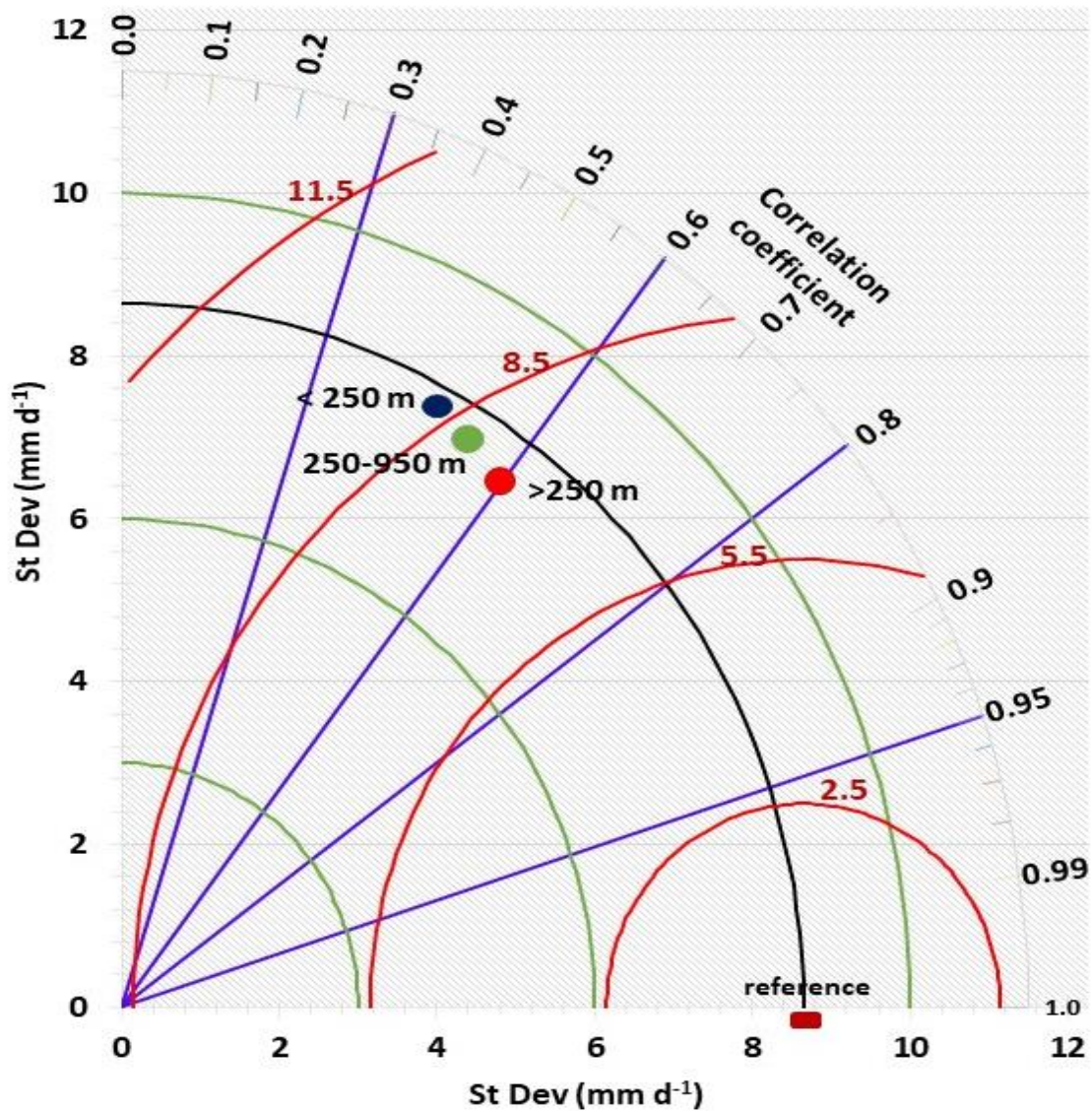


4
5 Figure 2: The spatial variation of bias (%) for gauge vs uncorrected CMORPH daily rainfall (1998-2013) for the Zambezi
6 Basin. The gauge-based isohyets for Mean Annual Precipitation (MAP) are shown in blue.

7 4.1. Effects of elevation and distance from large-scale open water bodies on CMORPH 8 bias

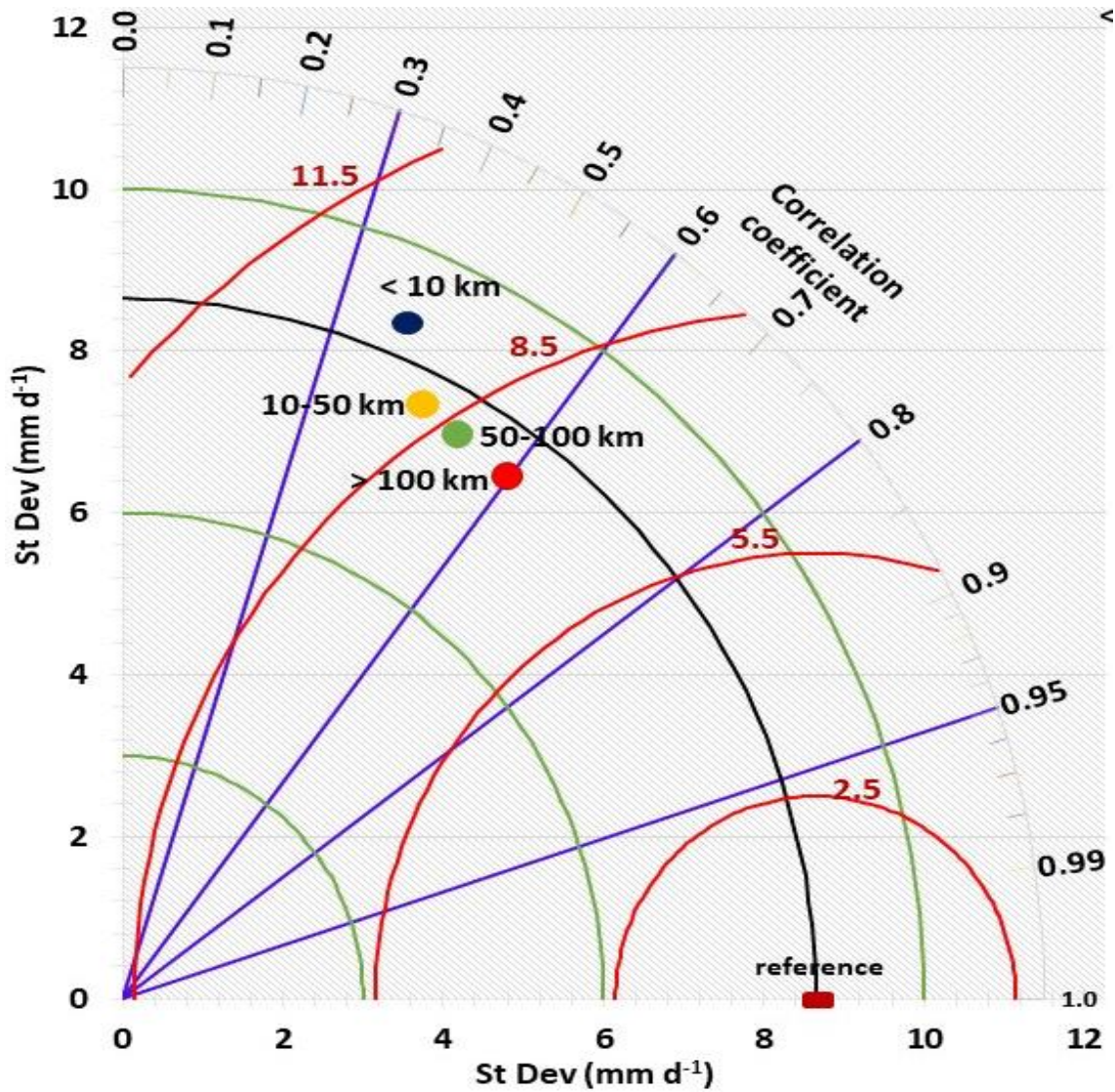
9 Figure 3 shows Taylor diagrams with a comparison of basin lumped estimates of daily
10 uncorrected time series (1999–2013) of CMORPH and gauge-based rainfall for the 3 elevation
11 zones (Figure 3a) and 4 distance zones from large-scale open water bodies (Figure 3b). Here
12 CMORPH performance is indicated by means of the root mean square difference (E),
13 correlation coefficient (R) and standard deviation. Figures 3a and 3b show that standard
14 deviations in the elevation zones and the distance zones (except for the < 10 km distance zone)
15 are lower than the reference/rain gauge standard deviation which is indicated by the black arc
16 (value of 8.45 mm d^{-1}). The stations in the high elevation zone (> 950 m) and long-distance
17 zone (> 100 km) reveal lower variability than stations at lower elevation and shorter distance
18 zones. With respect to the reference line, CMORPH estimates that are lumped for respective
19 elevation zones and distance to a large water body do not match standard deviation of rain
20 gauge-based counterparts. Figure 3a and 3b also show that CMORPH standard deviations that
21 are close to gauge-based rainfall apply to lower elevation and shorter distance zones. Based on

1 the Taylor diagrams, the statistics (R and E) for uncorrected CMORPH show increasing
 2 performance for increasing elevation and increasing distance from large-scale water bodies.
 3 Specifically, stations in the lower elevation zones (< 250m) have lower R and higher E than the
 4 higher elevation zones (> 950 m). For shorter distance zones lower R and higher E is shown
 5 than for longer distance zones (> 100 km). These findings suggest that in general effects of
 6 distance to large scale water body are minimal except for distances <10 km.



7
 8 Figure 3a. Elevation zones

9
 10



1

2 Figure 3b. Distance zones

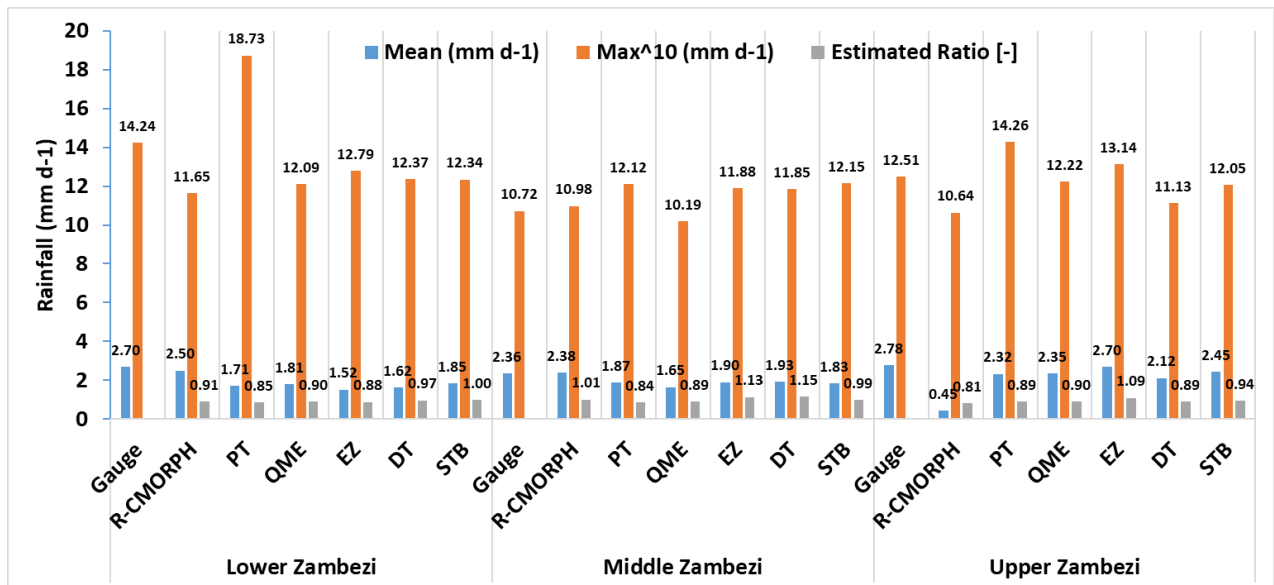
Figure 3. Time series of rain gauge (reference) vs CMORPH estimations, period 1999-2013, for elevation zones (Figure 3a) and distance zones (Figure 3b) in the Zambezi Basin. The correlation coefficients for the radial line denote the relationship between CMORPH and gauge-based observations. Standard deviations on both the x and y axes show the amount of variance between the two time series. The standard deviation of the CMORPH pattern is proportional to the radial distance from the origin. The angle between symbol and abscissa measures the correlation between CMORPH and rain gauge observations. The root mean square difference (red contours) between the CMORPH and rain gauge patterns is proportional to the distance to the point on the x-axis identified as "reference". For details, see Taylor (2001).

3 4.2. Evaluation of bias correction

4 4.2.1. Standard statistics

5 Figure 4 shows frequency-based statistics (mean and maximum) on accuracy of CMORPH
 6 rainfall estimates for each bias correction method. The ratio of cumulated estimates (1999-
 7 2013) from rain gauge and CMORPH estimates for the Lower, Middle and Upper Zambezi
 8 sub-basins are shown. Results show that the bias of CMORPH moderately reduced for each of
 9 the five bias correction schemes. However, the effectiveness of the schemes varies spatially

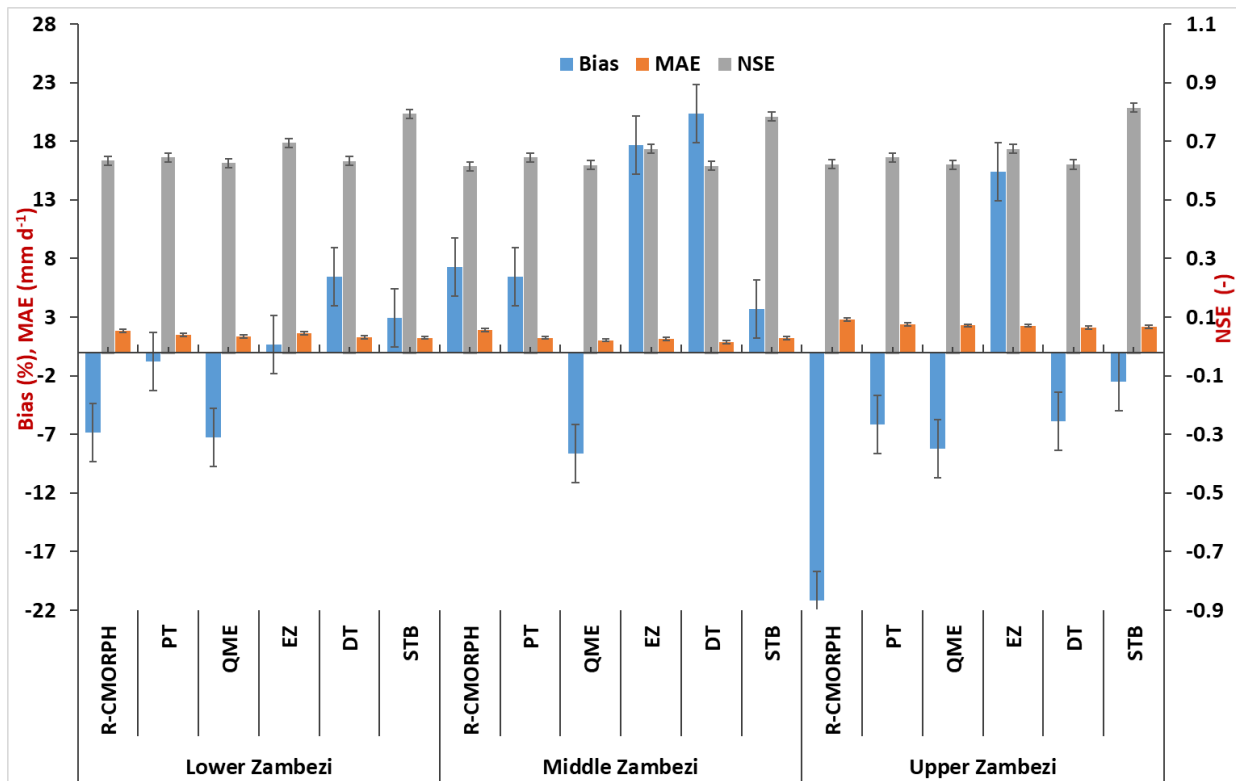
1 with best performance in Lower and Upper Zambezi sub-basin and relatively poor performance
 2 in the Middle Zambezi sub-basin (see Figure 4).



3
 4 Figure 4: Frequency based statistics (mean, max and estimated ratio of gauged sum vs CMORPH sum for 1999-2013) of
 5 corrected CMORPH for Lower, Middle and Upper Zambezi Basin.

6 Judging by the three performance indicators (mean, max and estimated ratio), results indicate
 7 that STB bias correction scheme is consistently effective in removing CMORPH rainfall bias
 8 in the Zambezi Basin. STB and PT effectively adjust for the mean of CMORPH rainfall
 9 estimates. Statistics in Figure 5 confirm these findings especially for the Upper Zambezi sub-
 10 basin where the mean of corrected estimates improved by > 60 % from the mean of uncorrected
 11 estimates. In addition, PT in the Lower Zambezi, QME in both Middle and Upper Zambezi and
 12 STB in the Upper Zambezi were also effective (improvement by 16 %) in correcting for the
 13 highest values in the rainfall estimates. STB performs better than other bias schemes in
 14 reproducing rainfall for the Lower and Upper Zambezi sub-basin, where the ratio of gauge total
 15 to corrected CMORPH total is close to 1.0.

16 Figure 5 shows the mean absolute error (MAE) and percentage bias (% bias) on the left axis
 17 and Nash Sutcliffe Efficiency (NSE) on the right axis as measures to evaluate performance of
 18 bias correction schemes in the Zambezi Basin. The effectiveness of the bias correction by all
 19 schemes varies over the different parts of the basin but is higher in the Lower and Upper
 20 Zambezi than in the Middle Zambezi. The STB, PT and EZ shows improved performance by
 21 exhibiting smaller MAEs compared to the uncorrected CMORPH (R-CMORPH). A greater
 22 improvement is shown for the Middle Zambezi where the uncorrected MAE of 1.89 mm d⁻¹ is
 23 reduced to 0.86 mm d⁻¹ after bias correction by the elevation zone bias correction scheme (EZ).
 24 The signal on improved performance for the Lower and Middle Zambezi as compared to the
 25 Upper Zambezi is also evident for the majority of the bias correction techniques. However,
 26 relatively large error remains in the MAE.



1

2 Figure 5: Percentage bias, Mean Absolute Error (left axis) and Nash Sutcliffe (NSE) (right axis) of corrected and uncorrected
 3 CMORPH (R-CMORPH) daily rainfall averaged for the Lower Zambezi, Middle Zambezi and Upper Zambezi for 1999-2013
 4 period.

5 NSE for STB is larger than 0.8 for all three Zambezi sub-basins. This is followed by EZ with
 6 NSE larger than 0.7 for the three sub-basins. The lowest NSE is for QME which is close to
 7 0.65 for all three sub-basins. Best results for reducing bias (% bias) are obtained by EZ in the
 8 Lower Zambezi (% bias of 0.7 % ~ absolute bias of 0.10 mm d⁻¹) and Upper Zambezi (0.22 %
 9 ~0.23 mm d⁻¹), PT in the Lower and Middle Zambezi (-0.84 % ~0.18 mm d⁻¹) and STB in all
 10 the basins (< 3.70 % ~0.24 mm d⁻¹). Gao and Liu (2013) over the Tibetan Plateau asserts that
 11 EZ is valuable in correcting systematic biases to provide a more accurate precipitation input
 12 for rainfall-runoff modelling. Significant underestimation for the uncorrected (-21.16 % ~0.44
 13 mm d⁻¹) and for bias corrected CMORPH are shown for the Upper Zambezi sub-basin.

14 4.2.2. Significance testing

15 Table 2 shows results of statistical tests to assess whether there is a significant difference ($p <$
 16 0.05) between rain gauge vs uncorrected and bias corrected CMORPH satellite rainfall for each
 17 of the 52 rain gauge stations. Results are summarised for the Upper, Middle and Lower
 18 Zambezi and in the Zambezi basin. The null hypothesis is rejected for PT (Lower Zambezi),
 19 DT (Upper Zambezi) and QME (all the 3 sub-basins) since $p < 0.05$. This means that
 20 statistically the above-mentioned bias correction schemes results deviate from the gauge. The
 21 null hypothesis is accepted for STB and EZ (all three sub-basins), DT (Lower and Upper
 22 Zambezi) and PT (Middle and Upper Zambezi), since $p > 0.05$ showing the effectiveness of

1 these bias correction schemes. Compared to uncorrected satellite rainfall (R-MORPH), results
 2 also reveal that the bias corrected satellite rainfall is closer to the gauge-based rainfall.

3 Table 2: Paired t-tests for the Upper, Middle and Lower Zambezi. The mean difference is significant at the 0.05 level. Bold
 4 shows significant values.

Basin	Rainfall Estimate	t-value	Mean Std. Error	p-value (0.05)
Lower Zambezi	R-CMORPH	8.95	0.04	0.04
	DT	39.86	0.09	0.35
	PT	21.08	0.04	0.03
	QME	23.99	0.04	0.04
	EZ	36.43	0.03	0.27
	STB	14.7	0.04	0.46
Middle Zambezi	R-CMORPH	3.27	0.03	0.001
	DT	41.9	0.07	0.24
	PT	26.02	0.03	0.14
	QME	18.38	0.03	0.00
	EZ	26.60	0.02	0.07
	STB	23.6	0.03	0.09
Upper Zambezi	R-CMORPH	4.28	0.08	0.00
	DT	22.63	0.14	0.01
	PT	12.98	0.07	0.05
	QME	13.27	0.07	0.00
	EZ	13.73	0.07	0.14
	STB	13.62	0.07	0.08

5

6 4.2.3. Analysis of variance (ANOVA test)

7 The ANOVA test is similar to a t-test except that the test was used to compare mean values
 8 from three or more data samples. Results of ANOVA shows that there is a significant ($p < 0.05$)
 9 difference in the mean values of the 5 bias correction results across the three sub-basins. This
 10 warranted the running of a post-hoc test to determine which schemes differ significantly. The
 11 contingency matrix in Table 3 shows results of the post-hoc test results summarized for the
 12 Tukey HSD, Scheffe and the Bonferroni methods but also for the Upper, Lower and Middle
 13 Zambezi. Table 3 also show that STB, PT and EZ are significantly different from the
 14 distribution transformation technique (DT) for the three sub-basins. STB, the best performing
 15 bias correction scheme identified using majority of the indicators, is also significantly different

1 from QME and EZ. QME which has poorly performed is significantly different from EZ.
 2 Results are important for further application of the bias correction schemes for studies such as
 3 flood, drought and water resources modelling.

4 Table 3: ANOVA post-hoc tests for the results of the five bias correction schemes ($p < 0.05$). The checklist table gives an
 5 indication (symbol) where two bias correction scheme's results are significantly different from each other. Where there is no
 6 symbol, it means that the schemes' results are not significantly different. The different symbols represent the Upper, Middle
 7 and Lower Zambezi basins.

	STB	PT	QME	DT	EZ
STB			✓	x ✓ ♀	✓
PT			♀	x ✓ ♀	
QME	✓				♀
DT	x ✓ ♀	x ✓ ♀	x ✓		x ♀
EZ	✓			x ✓ ♀	
	Key	x	Upper Zambezi		
		✓	Lower Zambezi		
		♀	Middle Zambezi		

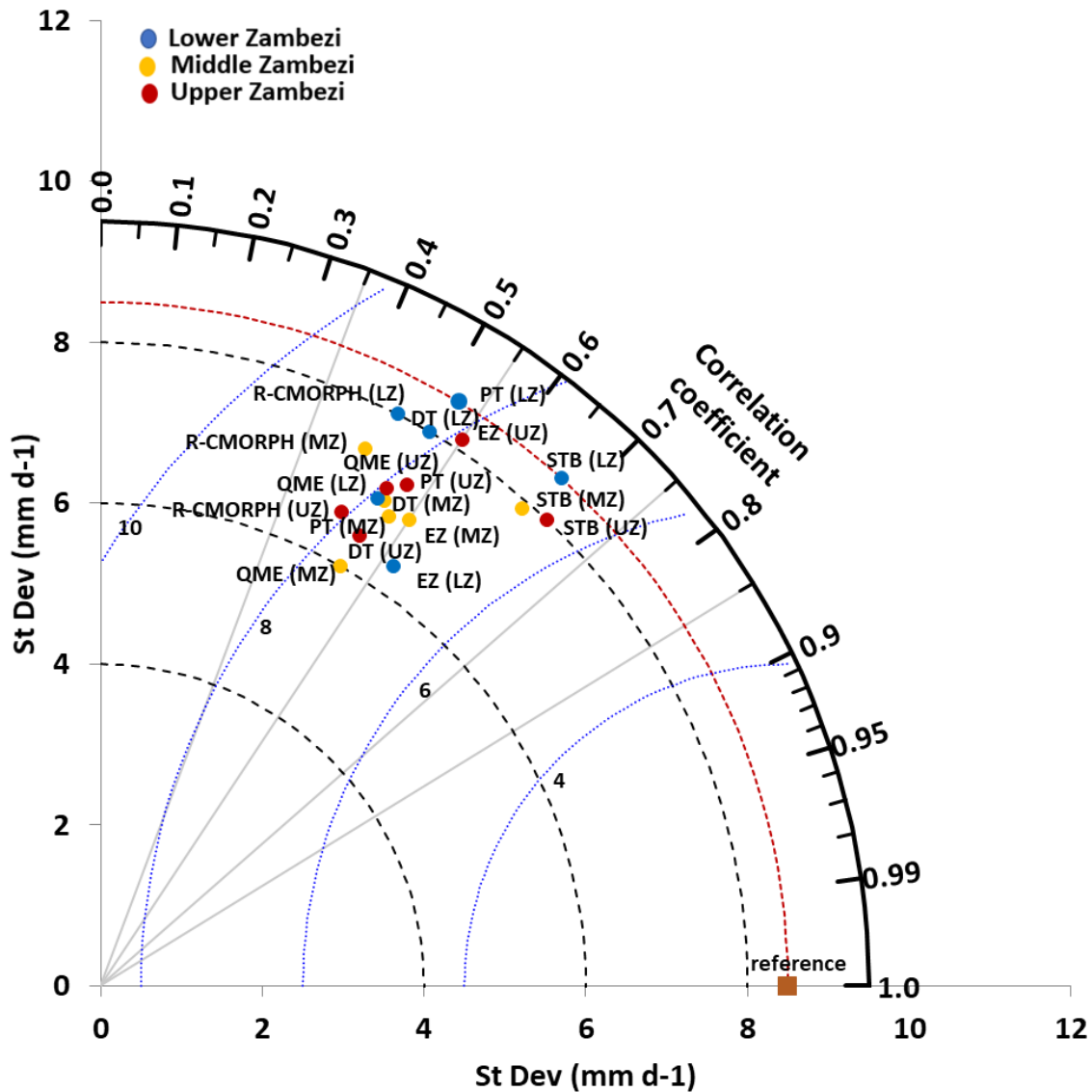
8

9 4.2.4. Taylor Diagrams

10 Figure 6 shows the Taylor diagram for time series of rain gauge (reference) observations vs
 11 CMORPH bias correction schemes averaged for the Lower Zambezi (UZ), Middle Zambezi
 12 (MZ) and Upper Zambezi (UZ). Absolute values used to develop the Taylor diagram are shown
 13 in Appendix 2. The position of each bias correction scheme and uncorrected satellite rainfall
 14 (R-MORPH) on Figure 6 shows how closely the rainfall by uncorrected CMORPH (R-
 15 MORPH) matches rain gauge observations as well as effectiveness of each of the bias schemes.
 16 Overall, all bias correction schemes show intermediate performance in terms of bias removal.
 17 Only the PT and STB for the Lower Zambezi sub-basin lie on the line of standard deviation
 18 (brown dashed arc) and means the standard deviation of the data for the two bias correction
 19 schemes match the gauge observations. This also indicates that rainfall variations after PT and
 20 STB bias correction for the Lower Zambezi resembles gauge based standard deviation. Note
 21 however that STB performs better than EZ as shown by the superior correlation coefficient.
 22 Compared against the reference line of mean standard deviation (8.5 mm d^{-1}), the rainfall
 23 standard deviation for most bias correction schemes is below this line and as such exhibit low
 24 variability across the Zambezi Basin.

25 Figure 6 also shows that most of the bias correction schemes have standard deviation range of
 26 6.0 to 8.0 mm d^{-1} . There is a consistent pattern between the bias correction schemes that have
 27 low R and high RMSE difference indicating that these schemes are not effective in bias
 28 removal. Overall, the best performing bias correction schemes (STB and EZ) have $R > 0.6$,
 29 standard deviation relatively close to the reference point and $\text{RMSE} < 7 \text{ mm d}^{-1}$. The
 30 uncorrected CMORPH (R-MORPH) lies far away from the marked reference (gauge) point on

1 the x-axis suggesting an intermediate overall effectiveness of the bias correction schemes such
 2 as STB, EZ, DT and PT in removing error as they are relatively closer to the marked reference
 3 point.



4
 5 Figure 6: Taylor's diagram on Rain gauge (reference) observations and CMORPH bias corrected estimates (all 5 schemes) as
 6 averaged for the Lower Zambezi (LZ), Middle Zambezi (MZ), and Upper Zambezi (UZ) for the period 1999-2013. The
 7 distance of the symbol from point (1, 0) is also a relative measure of the bias correction scheme performance. The position of
 8 each symbol appearing on the plot quantifies how closely precipitation estimates by respective bias correction scheme's
 9 matches counterparts by rain gauge. The dashed blue lines indicate the root mean square difference (mm d⁻¹).

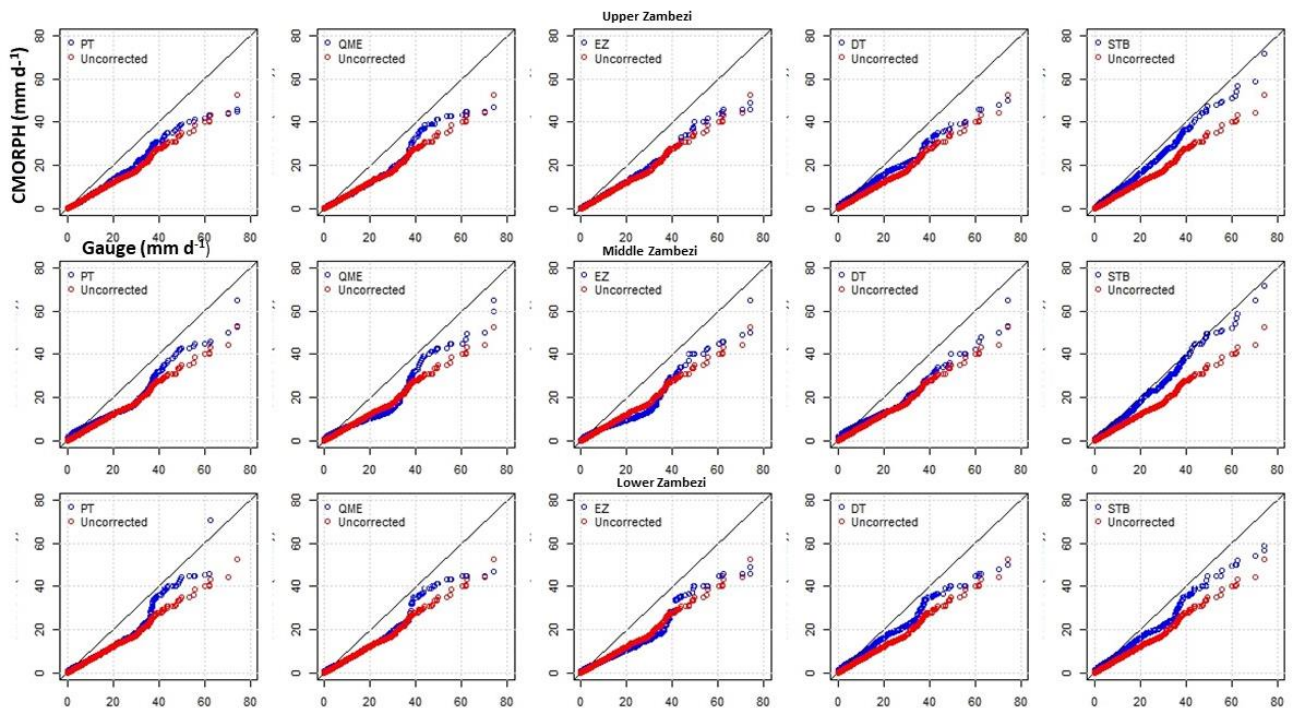
10 The least performing bias correction scheme is QME with relatively large RSMD (> 8 mm d⁻¹)
 11 and with low R (< 0.49) and standard deviation (< 6.5 mm d⁻¹). Inherent to the methodology
 12 of most of bias correction schemes (e.g. QME) is that the spatial pattern of the SRE does not
 13 change and therefore R for a specific station for daily precipitation does not necessarily
 14 improve. The bias correction results by the Taylor Diagram in Figure 6 corroborates with

1 findings shown in Figure 4 and Figure 5 for mean, max, ratio of rainfall totals and bias as
2 performance indicators.

3 4.2.5. *q-q plots*

4 Figure 7 shows q-q plots for the Upper, Middle and Lower Zambezi for gauge rainfall against
5 uncorrected and bias corrected CMORPH rainfall. Results show that STB's q-q plots for bias
6 corrected CMORPH across the 3 basins has majority of points that fall approximately along
7 the 45-degree reference line. This means that the STB bias corrected satellite rainfall has closer
8 distribution to the rain gauge as compared to the uncorrected CMORPH counterparts
9 suggesting effectiveness of the bias correction scheme. Other bias correction schemes such as
10 QME, EZ and PT have data points showing a greater departure from the 45-degree reference
11 line so performance is less effective.

12 In some instances, in both the Upper, Middle and Lower Zambezi, bias corrected values are
13 significantly higher than the corresponding gauge values whereas in some instances there is
14 serious underestimation. All q-q plots also show that for all bias correction schemes, the
15 differences between gauge and satellite rainfall are smallest for low rainfall rates ($< 2.5 \text{ mm d}^{-1}$)
16 and increasing for very heavy rainfall ($> 20.0 \text{ mm d}^{-1}$). In more detail, all the bias correction
17 schemes show a larger difference for the transition area from low to heavy rainfall. QME and
18 PT are not in good agreement with the rest of the bias correction schemes for higher rainfall
19 estimates ($40 \text{ and } 60 \text{ mm d}^{-1}$).



20

21 Figure 7: q-q plot for gauge vs satellite rainfall (uncorrected and bias corrected) for the Upper (top panes), Middle
22 (middle panes) and Lower (bottom panes) Zambezi.

1 4.2.6. CMORPH rainy days

2 Occurrence (%) of rainfall rates in the Zambezi Basin for each bias correction scheme is shown
 3 in Figure 8. The highest percentage (80-90 %) is shown for very light rainfall (0.0-2.5 mm d⁻¹).
 4 A smaller percentage is shown for 2.5-5.0 mm d⁻¹ which is the light rainfall class. Smallest
 5 percentage (< 5 %) is shown for very heavy rainfall (> 20 mm d⁻¹). The CMORPH rainfall
 6 corrected with STB, PT and DT matches the gauge-based rainfall (%) in the Lower, Middle
 7 and Upper Zambezi suggesting good performance. All five bias correction schemes in the
 8 Zambezi Basin generally tend to overestimate very light rainfall (< 2.5 mm d⁻¹). There is a
 9 small difference for moderate rainy days classification of 10.0-20.0 mm d⁻¹. For QME in the
 10 Middle and Upper Zambezi, there is overestimation by > 80 %. There is underestimation of
 11 rainfall greater than 20 mm d⁻¹.

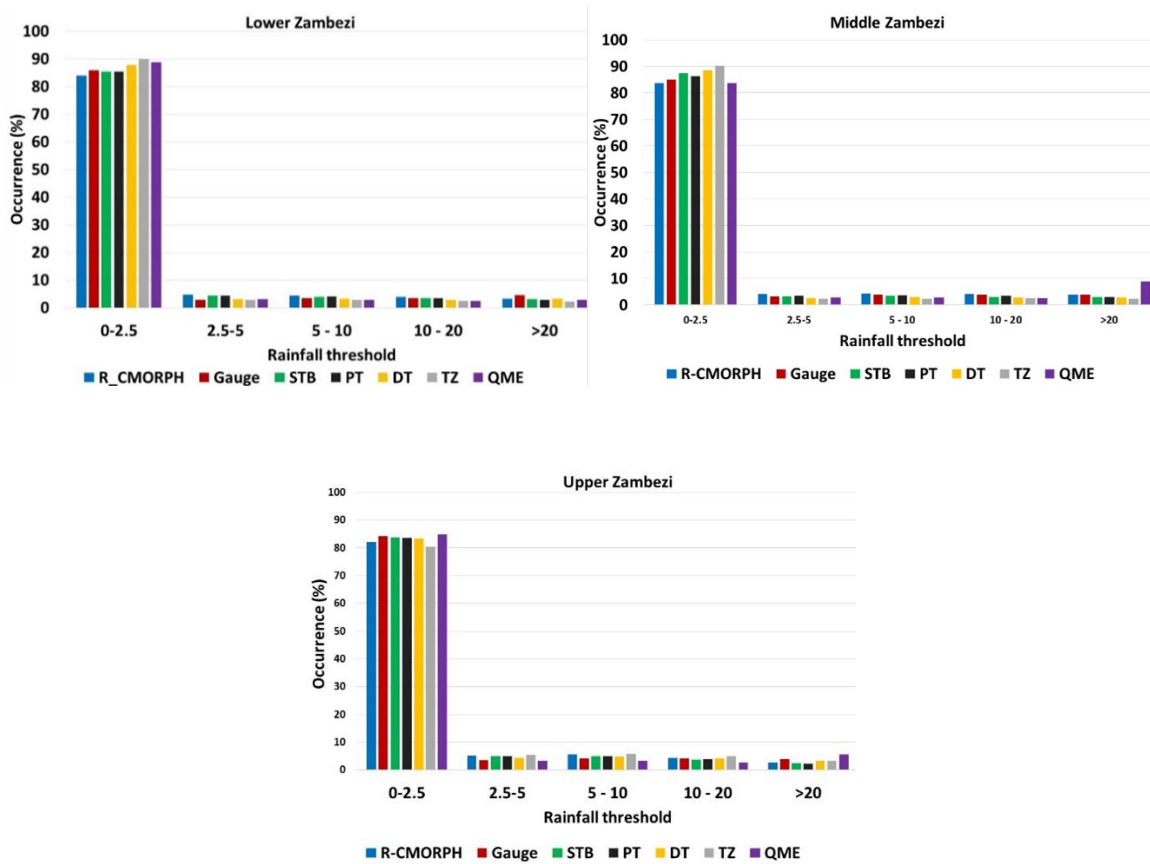


Figure 8: Percentage occurrence for rainfall rate classes

17 Figure 9 gives the bias correction performance for the different rainy-day classes. Results of
 18 bias removal varies for the Lower, Middle and Upper Zambezi. Comparatively, the STB and
 19 EZ show effectiveness in bias removal with an average bias correction of 0.97 % and 3.6 % in
 20 the whole basin respectively. Results show more effectiveness in reducing the percentage bias
 21 for light (2.5-5.0 mm d⁻¹) and moderate (5.0-10.0 mm d⁻¹) rainfall compared to the heavy (10.0-
 22 20.0 mm d⁻¹) and very heavy (> 20.0 mm d⁻¹) rainfall across the whole basin.

1



2

3

Figure 9: Bias correction (%) for respective rainfall rate (mm d^{-1}) classes

4

4.4. Spatial cross-validation

5

6

7

8

9

10

11

12

13

14

15

Table 4 shows the cross-validation results on bias correction for 8 rain gauge stations in the wet and dry seasons. It is evident that CMORPH has a considerable bias, although this bias is not always consistent for all 8 validation stations. Overall, Mutarara station has the highest positive bias (overestimation) whereas Makhanga has the highest negative bias (underestimation) for uncorrected CMORPH. Bias is effectively being removed by the STB followed by the EZ bias correction schemes. Bias is more effectively removed for the wet season than for the dry season. For the dry season, the STB shows good performance for Mkhanga and Nchalo stations, whereas good performance is shown for Kabompo and Chichiri stations. However, the MAE is higher for the wet season than for the dry season. Correlation coefficient for bias corrected satellite rainfall is higher for the wet season than for the dry season.

16

17

18

19

Table 4: Cross validation results for the bias correction procedure with 8 gauging stations for the dry and wet season. Stations lie at average elevation zone and sort of centred in an elevation zone. R-CMORPH is the uncorrected R-CMOPRPH estimate. DT, PT, QME, EZ and STB are the bias corrected rainfall estimate. Bold values indicate best performance. * = zone 1: elevation of < 250 m, ** = zone 2: elevation range of 250 - 950 m and *** = zone 3: elevation > 950 m

Dry Season (April-Sept)

Wet Season (Oct-March)

Station	Rainfall Estimate	Bias (%)	MAE mm d ⁻¹	Correlation	Estimated Ratio	Bias (%)	MAE (mm d ⁻¹)	Correlation
Makhanga*	R-CMORPH	-28.69	1.23	0.42	0.87	-21.17	8.63	0.43
	DT	-1.37	0.53	0.56	0.99	-1.66	3.96	0.65
	PT	-5.62	0.52	0.54	0.95	-3.5	4.67	0.64
	QME	1.98	0.54	0.54	0.95	-0.64	4.86	0.65
	EZ	2.10	0.47	0.55	1.03	-0.11	4.08	0.58
	STB	0.77	0.61	0.56	1.04	0.5	5.06	0.62
Nchalo*	R-CMORPH	-33.05	1.13	0.42	0.84	-25.18	8.05	0.38
	DT	-0.23	0.73	0.56	0.96	-2.61	3.65	0.50
	PT	-4.28	0.68	0.54	0.93	-6.48	5.05	0.59
	QME	1.90	0.72	0.53	0.81	-0.56	5.29	0.53
	EZ	0.35	0.63	0.54	0.99	0.22	4.4	0.60
	STB	-0.43	0.73	0.58	0.96	-1.23	5.54	0.61
Rukomichi**	R-CMORPH	-23.05	0.93	0.42	0.86	-21.18	6.69	0.31
	DT	-0.23	0.90	0.56	0.94	-6.2	3.51	0.60
	PT	-4.28	0.73	0.54	0.93	-2.48	3.62	0.59
	QME	1.90	0.75	0.53	1.03	-0.56	3.88	0.54
	EZ	0.35	0.71	0.54	0.99	0.22	3.5	0.60
	STB	-0.43	0.76	0.58	0.94	-1.26	3.33	0.61
Mutarara**	R-CMORPH	20.15	0.24	0.49	1.10	20.1	2.34	0.50
	DT	11.4	0.18	0.60	1.03	8.7	1.23	0.63
	PT	8.4	0.12	0.55	0.91	4.3	1.28	0.68
	QME	5.7	0.14	0.63	1.1	8.1	1.4	0.65
	EZ	-12.8	0.09	0.54	0.95	1.9	1.23	0.69
	STB	4.5	0.14	0.53	1.1	2.1	1.33	0.73
Mfuwe**	R-CMORPH	40.2	0.28	0.45	0.85	35.4	6.4	0.48
	DT	2.9	0.62	0.53	0.96	4.6	3.9	0.62
	PT	3.7	0.22	0.55	0.92	7.9	5.25	0.65
	QME	3.9	0.30	0.55	0.93	5.4	5.68	0.64
	EZ	6.1	0.24	0.54	0.92	3.8	5.18	0.56
	STB	5.4	0.26	0.65	0.93	1.2	4.66	0.65
Kabombo***	R-CMORPH	25.3	0.70	0.44	0.95	24.3	3.8	0.48
	DT	7.7	0.32	0.51	0.96	5.7	3.5	0.62

	PT	9.2	0.13	0.54	1.10	8.7	3.0	0.64
	QME	2.7	0.32	0.62	1.10	2.8	3.2	0.63
	EZ	5.6	0.22	0.53	0.91	3.3	2.7	0.54
	STB	19	0.13	0.62	1.01	9.3	2.7	0.64
	R-CMORPH	34.5	1.56	0.47	0.8	-37.3	4.7	0.45
	DT	12.2	0.60	0.51	0.85	5.5	3.2	0.51
Chichiri***	PT	9.4	0.42	0.52	1.04	-7.8	4.1	0.54
	QME	8.4	0.92	0.56	1.05	-13.0	4.1	0.64
	EZ	-13	0.61	0.60	0.94	-9.9	4.2	0.60
	STB	3.2	0.45	0.63	0.98	-14.3	2.1	0.65
	R-CMORPH	41.5	0.90	0.47	1.06	42.3	5.4	0.48
	DT	16.7	0.53	0.54	0.98	-13.2	3.3	0.62
Chitedze***	PT	-16.5	0.44	0.55	0.99	22.2	4.5	0.65
	QME	18.2	0.41	0.57	1.04	18.5	4.3	0.64
	EZ	11.7	0.32	0.57	1.02	8.4	4.6	0.55
	STB	3.9	0.23	0.60	0.03	-8.2	3.7	0.65
	R-CMORPH	41.5	0.90	0.47	1.06	42.3	5.4	0.48

1

2 4.5. Temporal cross-validation

3 The same performance indicators in spatial cross-validation are calculated for the temporal
4 cross-validation. Results are presented in Table 5. The MAE is higher for the wet season than
5 for the dry season. The difference in effectiveness in the error removal between the dry and wet
6 season is much larger. STB outperforms both bias correction methods but does also have
7 problems correcting the estimated ratios. After the correction, the correlation coefficient is
8 much improved. The fact that MAE remains relatively large indicates that errors remain locally
9 large. These values are almost in same range to performance indicators obtained from the main
10 performance assessment period (1999-2013). The estimated ratio shows improvement for the
11 Middle Zambezi compared to the Lower and Upper Zambezi.

12 Table 5: Temporal-cross validation results for the period 1998-1999 for the wet and dry season

		Dry Season (April-Sept)				Wet Season (Oct-March)		
Rainfall Estimate		Bias (%)	MAE (mm d ⁻¹)	Correlation	Estimated Ratio	Bias (%)	MAE (mm d ⁻¹)	Correlation
Lower	R-CMORPH	-28.26	1.10	0.42	0.86	-22.51	7.79	0.37
Zambezi	DT	-0.61	0.72	0.56	0.96	-3.49	3.71	0.58

	PT	-4.73	0.64	0.54	0.94	-4.15	4.45	0.61
	QME	1.93	0.67	0.53	0.93	-0.59	4.68	0.57
	EZ	0.93	0.60	0.54	1.00	0.11	3.99	0.59
	STB	-0.03	0.70	0.57	0.98	-0.66	4.64	0.61
	R-CMORPH	28.55	0.41	0.46	0.97	26.60	4.18	0.49
	DT	7.33	0.37	0.55	0.98	6.33	2.88	0.62
Middle Zambezi	PT	7.10	0.16	0.55	0.98	6.97	3.18	0.66
	QME	4.10	0.25	0.60	1.04	5.43	3.43	0.64
	EZ	-0.37	0.18	0.54	0.93	3.00	3.04	0.60
	STB	9.63	0.18	0.60	1.01	4.20	2.90	0.67
	R-CMORPH	38	1.23	0.47	0.93	2.5	5.05	0.465
	DT	14.45	0.565	0.525	0.915	-3.85	3.25	0.565
Upper Zambezi	PT	-3.55	0.43	0.535	1.015	7.2	4.3	0.595
	QME	13.3	0.665	0.565	1.045	2.75	4.2	0.64
	EZ	-0.65	0.465	0.585	0.98	-0.75	4.4	0.575
	STB	3.55	0.34	0.615	0.505	-11.25	2.9	0.65

1

2 5. Discussion

3 We present methods to assess the performance of bias correction schemes for CMORPH
4 rainfall estimates in the Zambezi River Basin. For correction we applied sequential windows
5 of 7 days that count 5 rainy days with rainfall threshold of 5 mm d⁻¹. First, we aimed to evaluate
6 if performance of CMORPH rainfall is affected by elevation and distance from large scale open
7 water bodies. Results in Taylor diagrams show that effects of distances > 10 km are minimal
8 in this study. For distance < 10 km, results in the same Taylor diagrams shows some effect with
9 increased CMORPH estimation errors although not clearly identifiable by the limited number
10 of gauging stations at distance < 10 km. The low number of gauge stations constrains clear
11 identification of bias as effected by the short distance. The low number of stations also
12 constrains detailed analysis on dependencies of observation time series. To assess bias effects
13 at distances < 10 km we advocate installation of a well-designed network of rain gauges with
14 stations located at preselected locations that would allow sound geostatistical analysis on small
15 scale rainfall variability and spatial correlation analysis. We refer to (Ciach and Krajewski,
16 2006) who present such analysis for a dense experimental network of 53 stations. The inter-
17 station distance of the rain gauges in this study is too large to capture the effect of distance to
18 large scale open water bodies on CMORPH rainfall error. For instance, such distance exceeds
19 350 km for most of Upper Zambezi Basin. Findings in this study show that effects of distance

1 would be captured at distances 10-25 km or shorter. Haile et al. (2009) indicates bias effects at
2 short distances (<10 km) for the Lake Tana, Ethiopia.

3 The rainfall-elevation bias correction also shows minimal signal. Contrary to this finding,
4 Romilly and Gebremichael (2011) showed that the accuracy of CMORPH at monthly time base
5 is related to elevation for six river basins in Ethiopia. A similar finding was reported by Haile
6 et al. (2009), Katiraie-Boroujerdy et al., (2013) and Wu and Zhai (2012) who found that
7 performance of CMORPH is affected by elevation. However, Vernimmen et al. (2012)
8 concluded that TRMM Multi-satellite Precipitation Analysis (TMPA) 3B42RT performance
9 was not affected by elevation ($R^2 = 0.0001$) for Jakarta, Bogor, Bandung, Java, Kalimantan and
10 Sumatra regions (Indonesia). The study by Gao and Liu (2013) showed that the bias in
11 CMORPH rainfall over the Tibetan Plateau is affected by elevation. Whilst distance from large
12 scale open water bodies and elevation have been assessed separately for this study, Habib et al.
13 (2012a) revealed that both aspects interact in the Nile Basin to produce unique circulation
14 patterns to affect the performance of SRE.

15

16 Secondly, we evaluate the effectiveness of linear/non-linear and time-space variant/invariant
17 bias correction schemes. The bias correction results by means of performance indicators such
18 as Taylor Diagrams, q-q plots, ANOVA and standard statistics such as mean, max, ratio of
19 rainfall totals and bias reveal that the STB is the best bias correction method. This method by
20 its nature, consider correction only for spatial distributed patterns in bias, commonly known as
21 space variant/invariant and thus forces the estimates to behave as observations. We did not
22 investigate effects of the applied sequential windows of 7 days for each bias correction scheme
23 separately but note that other window lengths possibly could yield more favourable results for
24 bias schemes such as PT, DT and QME that commonly rely on larger sample sizes. As alluded
25 to by Habib (2013), correction should improve hydrological applications by improved rainfall
26 representation. This applies to Zambezi basin as well with demands for applications of the
27 product such as for drought analysis, flood prediction, weather forecasting and rainfall-runoff
28 modelling. The study is unique as we assess the importance of space and time aspects of
29 CMORPH bias for rainfall-runoff modeling in a data scarce catchment. Findings in this study
30 on cross and temporal validation contribute to efforts that aim towards enhancing applications
31 of satellite rainfall products. The study site is the Zambezi Basin, an example of many world
32 regions that can benefit from satellite-based rainfall products for resource assessments and
33 monitoring.

34 Thirdly, an assessment of the performance of bias correction schemes to represent different
35 rainfall rates and climate seasonality is presented. Our findings show that bias is most
36 overestimated for the very light rainfall (< 2.5 mm d⁻¹), which is also the range that shows the
37 best bias reduction, which in turn is most effective during the wet season. Results also show
38 that there is underestimation of rainfall larger than 20 mm d⁻¹. The poor performance of
39 correction for the heavy rainfall class is caused by, sometimes, large mismatch of high rain

1 gauge values versus low CMORPH values. This leads to unrealistically high CMORPH values
2 which remain poorly corrected by bias schemes. Results are consistent with findings by Gao
3 and Liu (2013) in the Tibetan Plateau who found consistent under and overestimation of
4 occurrence by CMORPH for rainfall rates $>10 \text{ mm d}^{-1}$. A study by Zulkafli et al. (2014) in
5 French Guiana and North Brazil noted that the low sampling frequency and consequently
6 missed short-duration precipitation events between satellite measurements results in
7 underestimation, particularly for rainfall $> 20 \text{ mm d}^{-1}$.

8 Lastly, spatial and temporal cross validation reveal effectiveness of bias correction schemes.
9 The hold-out sample of 8 stations in this work showed the applicability of different bias
10 correction methods under different geographical domains. There is improved performance of
11 satellite rainfall for the wet season than for the dry season based on correlation coefficient and
12 MAE. The study by Ines and Hansen (2006) for semi-arid eastern Kenya showed that
13 multiplicative bias correction schemes such as STB were effective in correcting the total of the
14 daily rainfall grouped into seasons. Our results show that effectiveness in bias removal in the
15 wet season is higher than in the dry season. This is contrary to Vernimmen et al. (2012) who
16 showed that for the dry season, bias for PT decreased in Jakarta, Bogor, Bandung, East Java
17 and Lampung regions after bias correction of monthly TMPA 3B42RT precipitation estimates
18 over the period 2003–2008. Habib (2014) evaluated sensitivity of STB for the dry and wet
19 season and concluded that the bias correction factor for CMOPRH shows lower sensitivity for
20 the wet season as compared to the dry season. Our findings also reveal that bias factors for all
21 the schemes are more variable in the dry season than in the wet season and lead to poor
22 performance of the bias correction schemes in the dry season.

23 **6. Conclusions**

24 In this study four conclusions are drawn:

- 25 1. Analysis on gauge and CMORPH rainfall estimates shows that performance increases for
26 higher elevation ($> 950 \text{ m}$) in the Zambezi Basin and that CMORPH has largest mismatch
27 at low elevation. Such analysis was established for rain gauges within elevation classes of
28 $< 250 \text{ m}$, $250 - 950 \text{ m}$ and $> 950 \text{ m}$. The match between gauge and CMORPH estimates
29 improved at increasing distance to large-scale open water bodies. This was established for
30 rain gauges located within specified distances of $10 - 50 \text{ km}$, $50 - 100 \text{ km}$ and $> 100 \text{ km}$ to
31 a large-scale open water body. For distances $< 10 \text{ km}$ errors by CMORPH increased but the
32 small sample size of stations and the weak signal require further study. To assess how bias
33 is affected at short distance to a large-scale water body, a specifically designed and dense
34 gauging network is s are advocated (see Ciach and Krajewski, 2006) that allow evaluation
35 of small-scale rainfall variability. A detailed analysis on small spatial variability and spatial
36 correlation analysis of rain gauged observations presumably is prerequisite before satellite
37 rainfall effects at short distance to a large-scale water body can be assessed.

- 1 2. For each of the five bias correction methods applied, accuracy of the CMORPH satellite
2 rainfall estimates improved. Assessment through standard statistics, Taylor Diagrams, t-
3 tests, ANOVA and q-q plots shows that STB that accounts for space and time variation of
4 bias, is found more effective in reducing rainfall bias in the basin than the rest of the bias
5 correction schemes. This indicates that the temporal aspect of CMORPH bias is more
6 important than the spatial aspect in the Zambezi Basin. Quantile-quantile (q-q) plots for all
7 the bias correction schemes in general show that bias corrected rainfall is in good agreement
8 with gauge-based rainfall for low rainfall rates but that high rainfall rates are largely
9 overestimated.
- 10 3. Differences in the mechanisms that drive precipitation throughout the year could result in
11 different biases for each of the seasons, which motivated us to calculate the bias correction
12 factors for dry and wet seasons separately. As such CMORPH rainfall time series were
13 divided to assess the influence of seasonality on performance of bias correction schemes.
14 Overall, the bias correction schemes reveal that bias removal is more effective in the wet
15 season than in the dry season.
- 16 4. We assessed whether bias correction varies for different rainfall rates of daily rainfall in the
17 Zambezi Basin. There is overestimation of very light rainfall ($< 2.5 \text{ mm d}^{-1}$) and
18 underestimation of very heavy rainfall ($>20 \text{ mm d}^{-1}$) after application of the bias correction
19 schemes. Bias was more effectively reduced for the very light ($< 2.5 \text{ mm d}^{-1}$), to moderate
20 ($5.0\text{-}10.0 \text{ mm d}^{-1}$) rainfall compared to the heavy ($10.0\text{-}20.0 \text{ mm d}^{-1}$) and very heavy (> 20
21 mm d^{-1}) rainfall. Overall, the STB and EZ more consistently removed bias in all the rainy
22 days classification compared to the three other bias correction schemes. Effects of length
23 of sequential window sizes for selected bias correction schemes is not investigated but
24 different length possibly could yield more favourable results for PT, QME and DT bias
25 correction schemes.

26 Analysis serve to improve reliability of SREs applications in hydrological analysis and water
27 resource applications in the Zambezi basin such as in drought analysis, flood prediction,
28 weather forecasting and rainfall runoff modelling. In follow-up studies, we aim at hydrologic
29 evaluation of bias corrected CMORPH rainfall estimates at the headwater catchment of the
30 Zambezi River.

31 **Data availability**

32 Supplementary data consists of shapefiles of the Zambezi study area boundary, sub-basin
33 boundaries, location of the 60 rain gauges and lakes (Figure 1). Additional material provided
34 is the raster files of uncorrected CMORPH bias (%) making up Figure 2. Raster files of daily
35 and yearly uncorrected CMORPH and gauge rainfall from 1998-2013 are also provided.

36 **Acknowledgements**

1 The study was supported by WaterNet through the DANIDA Transboundary PhD Research in
2 the Zambezi Basin and the University of Twente's ITC Faculty. The authors acknowledge the
3 University of Zimbabwe's Civil Engineering Department for platform to carry out this
4 research.

5 **Author Contributions**

6 Webster Gumindoga was responsible for the development of bias correction schemes in the
7 Zambezi basin and research approach. Tom Rientjes and Alemseged Haile were responsible for
8 synthesising the methodology and made large contributions to the manuscript write-up. Hodson
9 Makurira provided some of the rain gauge data and related findings of this study to previous
10 work in the Zambezi Basin. Reggiani Paolo assisted in interpretation of bias correction results.

11 **Conflict of Interests**

12 The authors declare no conflict of interests.

13 **References**

- 14 Beilfuss, R., Dutton, P., and Moore, D.: Landcover and Landuse change in the Zambezi Delta,
15 in: Zambezi Basin Wetlands Volume III Landuse Change and Human impacts, Chapter
16 2, Biodiversity Foundation for Africa, Harare, 31-105, 2000.
- 17 Beilfuss, R.: A Risky Climate for Southern African Hydro: Assessing hydrological risks and
18 consequences for Zambezi River Basin dams, 2012.
- 19 Beyer, M., Wallner, M., Bahlmann, L., Thiemig, V., Dietrich, J., and Billib, M.: Rainfall
20 characteristics and their implications for rain-fed agriculture: a case study in the Upper
21 Zambezi River Basin, Hydrological Sciences Journal, null-null,
22 10.1080/02626667.2014.983519, 2014.
- 23 Bitew, M. M., and Gebremichael, M.: Evaluation of satellite rainfall products through
24 hydrologic simulation in a fully distributed hydrologic model, Water Resources
25 Research, 47, 2011.
- 26 Bitew, M. M., Gebremichael, M., Ghebremichael, L. T., and Bayissa, Y. A.: Evaluation of High-
27 Resolution Satellite Rainfall Products through Streamflow Simulation in a
28 Hydrological Modeling of a Small Mountainous Watershed in Ethiopia, Journal of
29 Hydrometeorology, 13, 338-350, 10.1175/2011jhm1292.1, 2011.
- 30 Bouwer, L. M., Aerts, J. C. J. H., Van de Coterlet, G. M., Van de Giessen, N., Gieske, A., and
31 Manaerts, C.: Evaluating downscaling methods for preparing Global Circulation Model
32 (GCM) data for hydrological impact modelling. Chapter 2, in Aerts, J.C.J.H. &
33 Droogers, P.

- 1 Brown, A. M.: A new software for carrying out one-way ANOVA post hoc tests, *Comput.*
2 *Methods Programs Biomed.*, 79(1), 89–95,
3 doi:<https://doi.org/10.1016/j.cmpb.2005.02.007>, 2005.
- 4 (Eds.), *Climate Change in Contrasting River Basins: Adaptation Strategies for Water, Food and*
5 *Environment*. (pp. 25-47). Wallingford, UK: Cabi Press., 2004.
- 6 Cecinati, F., Rico-Ramirez, M. A., Heuvelink, G. B. M., and Han, D.: Representing radar
7 rainfall uncertainty with ensembles based on a time-variant geostatistical error
8 modelling approach, *Journal of Hydrology*, 548, 391-405,
9 <http://dx.doi.org/10.1016/j.jhydrol.2017.02.053>, 2017.
- 10 Ciach, G. J. and Krajewski, W. F.: Analysis and modeling of spatial correlation structure in
11 small-scale rainfall in Central Oklahoma, *Adv. Water Resour.*, 29(10), 1450–1463,
12 doi:<https://doi.org/10.1016/j.advwatres.2005.11.003>, 2006.
- 13 Cohen Liechti, T., Matos, J. P., Boillat, J. L., and Schleiss, A. J.: Comparison and evaluation of
14 satellite derived precipitation products for hydrological modeling of the Zambezi River
15 Basin, *Hydrol. Earth Syst. Sci.*, 16, 489-500, 2012.
- 16 Cuvelier, C., Thunis, P., Vautard, R., Amann, M., Bessagnet, B., Bedogni, M., Berkowicz, R.,
17 Brandt, J., Brocheton, F., Builtjes, P., Carnavale, C., Coppalle, A., Denby, B., Douros,
18 J., Graf, A., Hellmuth, O., Hodzic, A., Honoré, C., Jonson, J., Kerschbaumer, A., de
19 Leeuw, F., Minguzzi, E., Moussiopoulos, N., Pertot, C., Peuch, V. H., Pirovano, G.,
20 Rouil, L., Sauter, F., Schaap, M., Stern, R., Tarrason, L., Vignati, E., Volta, M., White,
21 L., Wind, P., and Zuber, A.: CityDelta: A model intercomparison study to explore the
22 impact of emission reductions in European cities in 2010, *Atmospheric Environment*,
23 41, 189-207, <http://dx.doi.org/10.1016/j.atmosenv.2006.07.036>, 2007.
- 24 Dennis, R., Fox, T., Fuentes, M., Gilliland, A., Hanna, S., Hogrefe, C., Irwin, J., Rao, S. T.,
25 Scheffe, R., Schere, K., Steyn, D., and Venkatram, A.: A framework for evaluating
26 regional-scale numerical photochemical modeling systems, *Environmental Fluid*
27 *Mechanics*, 10, 471-489, [10.1007/s10652-009-9163-2](https://doi.org/10.1007/s10652-009-9163-2), 2010.
- 28 Dinku, T., Chidzambwa, S., Ceccato, P., Connor, S. J., and Ropelewski, C. F.: Validation of
29 high-resolution satellite rainfall products over complex terrain, *International Journal*
30 *of Remote Sensing*, 29, 4097-4110, [10.1080/01431160701772526](https://doi.org/10.1080/01431160701772526), 2008.
- 31 Fang, G. H., Yang, J., Chen, Y. N., and Zammit, C.: Comparing bias correction methods in
32 downscaling meteorological variables for a hydrologic impact study in an arid area in
33 China, *Hydrol. Earth Syst. Sci.*, 19, 2547-2559, [10.5194/hess-19-2547-2015](https://doi.org/10.5194/hess-19-2547-2015), 2015.
- 34 Field, A.: *Discovering statistics using SPSS 2nd ed.* Sage Publications, 2009.

- 1 Fylstra, D., Lasdon, L., Watson, J., and Waren, A.: Design and Use of the Microsoft Excel
2 Solver, Interfaces, 28, 29-55, doi:10.1287/inte.28.5.29, 1998.
- 3 Gao, Y. C., and Liu, M. F.: Evaluation of high-resolution satellite precipitation products using
4 rain gauge observations over the Tibetan Plateau, Hydrol. Earth Syst. Sci., 17, 837-849,
5 10.5194/hess-17-837-2013, 2013.
- 6 Gebregiorgis, A. S., Tian, Y., Peters-Lidard, C. D., and Hossain, F.: Tracing hydrologic model
7 simulation error as a function of satellite rainfall estimation bias components and land
8 use and land cover conditions, Water Resources Research, 48, n/a-n/a,
9 10.1029/2011wr011643, 2012.
- 10 Grillakis, M. G., Koutroulis, A. G., Daliakopoulos, I. N., and Tsanis, I. K.: A method to preserve
11 trends in quantile mapping bias correction of climate modeled temperature, Earth Syst.
12 Dynam. Discuss., 2017, 1-26, 10.5194/esd-2017-53, 2017.
- 13 Gumindoga, W., Rientjes, T. H. M., Haile, A. T., Makurira, H., and Reggiani, P.: Performance
14 evaluation of CMORPH satellite precipitation product in the Zambezi Basin,
15 International Journal of Remote Sensing, 1-20, [10.1080/01431161.2019.1602791](https://doi.org/10.1080/01431161.2019.1602791).
- 16 Gutjahr, O. and Heinemann, G.: Comparing precipitation bias correction methods for high-
17 resolution regional climate simulations using COSMO-CLM, Theor. Appl. Climatol.,
18 114(3-4), 511-529, doi:10.1007/s00704-013-0834-z, 2013.
- 19 Habib, E., ElSaadani, M., and Haile, A. T.: Climatology-Focused Evaluation of CMORPH and
20 TMPA Satellite Rainfall Products over the Nile Basin, Journal of Applied Meteorology
21 and Climatology, 51, 2105-2121, 10.1175/jamc-d-11-0252.1, 2012a.
- 22 Habib, E., Haile, A. T., Tian, Y., and Joyce, R. J.: Evaluation of the High-Resolution CMORPH
23 Satellite Rainfall Product Using Dense Rain gauge Observations and Radar-Based
24 Estimates, Journal of Hydrometeorology, 13, 1784-1798, 10.1175/jhm-d-12-017.1,
25 2012b.
- 26 Habib, E., Haile, A., Sazib, N., Zhang, Y., and Rientjes, T.: Effect of Bias Correction of
27 Satellite-Rainfall Estimates on Runoff Simulations at the Source of the Upper Blue
28 Nile, Remote Sensing, 6, 6688-6708, 2014.
- 29 Haile, A. T., Rientjes, T., Gieske, A., and Gebremichael, M.: Rainfall Variability over
30 Mountainous and Adjacent Lake Areas: The Case of Lake Tana Basin at the Source of
31 the Blue Nile River, Journal of Applied Meteorology and Climatology, 48, 1696-1717,
32 10.1175/2009JAMC2092.1, 2009.
- 33 Haile, A. T., Habib, E., and Rientjes, T. H. M.: Evaluation of the climate prediction center CPC
34 morphing technique CMORPH rainfall product on hourly time scales over the source
35 of the Blue Nile river, Hydrological processes, 27, 1829-1839, 2013.

- 1 Haile, A. T., Yan, F., and Habib, E.: Accuracy of the CMORPH satellite-rainfall product over
2 Lake Tana Basin in Eastern Africa, Atmospheric Research. *In Press, Accepted*
3 *manuscript*, <http://dx.doi.org/10.1016/j.atmosres.2014.11.011>, 2014.
- 4 Haile, A. T., Yan, F., and Habib, E.: Accuracy of the CMORPH satellite-rainfall product over
5 Lake Tana Basin in Eastern Africa, Atmospheric Research, 163, 177-187,
6 <http://dx.doi.org/10.1016/j.atmosres.2014.11.011>, 2015.
- 7 Heidinger, H., Yarlequé, C., Posadas, A., and Quiroz, R.: TRMM rainfall correction over the
8 Andean Plateau using wavelet multi-resolution analysis, International Journal of
9 Remote Sensing, 33, 4583-4602, 10.1080/01431161.2011.652315, 2012.
- 10 Hempel, S., Frieler, K., Warszawski, L., Schewe, J., and Piontek, F.: A trend-preserving bias
11 correction - the ISI-MIP approach, Earth Syst. Dynam., 4, 219-236, 10.5194/esd-4-219-
12 2013, 2013.
- 13 Hughes, D. A.: Comparison of satellite rainfall data with observations from gauging station
14 networks, Journal of Hydrology, 327, 399-410,
15 <http://dx.doi.org/10.1016/j.jhydrol.2005.11.041>, 2006.
- 16 Ines, A. V. M., and Hansen, J. W.: Bias correction of daily GCM rainfall for crop simulation
17 studies, Agricultural and Forest Meteorology, 138, 44-53,
18 <http://dx.doi.org/10.1016/j.agrformet.2006.03.009>, 2006.
- 19 Jiang, S.-h., Zhou, M., Ren, L.-l., Cheng, X.-r., and Zhang, P.-j.: Evaluation of latest TMPA and
20 CMORPH satellite precipitation products over Yellow River Basin, Water Science and
21 Engineering, 9, 87-96, <http://dx.doi.org/10.1016/j.wse.2016.06.002>, 2016.
- 22 Johnson, F. and Sharma, A.: Accounting for interannual variability: A comparison of options
23 for water resources climate change impact assessments, Water Resour. Res., 47(4),
24 doi:10.1029/2010WR009272, 2011.
- 25 Katiraie-Boroujerdy, P., Nasrollahi, N., Hsu, K., and Sorooshian, S.: Evaluation of satellite-
26 based precipitation estimation over Iran, Elsevier, Kidlington, ROYAUME-UNI, 15
27 pp., 2013.
- 28 Khan, S. I., Hong, Y., Gourley, J. J., Khattak, M. U. K., Yong, B., and Vergara, H. J.: Evaluation
29 of three high-resolution satellite precipitation estimates: Potential for monsoon
30 monitoring over Pakistan, Advances in Space Research, 54, 670-684,
31 <http://dx.doi.org/10.1016/j.asr.2014.04.017>, 2014.
- 32 Koutsouris, A. J., Chen, D., and Lyon, S. W.: Comparing global precipitation data sets in eastern
33 Africa: a case study of Kilombero Valley, Tanzania, Int. J. Climatol., 36, 2000-2014,
34 10.1002/joc.4476, 2016.

- 1 Kucuk, U., Eyuboglu, M., Kucuk, H. O. and Degirmencioglu, G.: Importance of using proper
2 post hoc test with ANOVA, *Int. J. Cardiol.*, 209, 346, doi:10.1016/j.ijcard.2015.11.061,
3 2018.
- 4 Leander, R., Buishand, T. A., van den Hurk, B. J. J. M. and de Wit, M. J. M.: Estimated changes
5 in flood quantiles of the river Meuse from resampling of regional climate model output,
6 *J. Hydrol.*, 351(3–4), 331–343, doi:10.1016/j.jhydrol.2007.12.020, 2008.
- 7 Lenderink, G., Buishand, A. and van Deursen, W.: Estimates of future discharges of the river
8 Rhine using two scenario methodologies: direct versus delta approach, *Hydrol. Earth
9 Syst. Sci.*, 11(3), 1145–1159, doi:10.5194/hess-11-1145-2007, 2007.
- 10 Li, J., and Heap, A. D.: A review of comparative studies of spatial interpolation methods in
11 environmental sciences: Performance and impact factors, *Ecological Informatics*, 6,
12 228-241, <http://dx.doi.org/10.1016/j.ecoinf.2010.12.003>, 2011.
- 13 Liu, J., Duan, Z., Jiang, J., and Zhu, A.-X.: Evaluation of Three Satellite Precipitation Products
14 TRMM 3B42, CMORPH, and PERSIANN over a Subtropical Watershed in China,
15 *Advances in Meteorology*, 2015, 13, 10.1155/2015/151239, 2015.
- 16 Liu, Z.: Comparison of precipitation estimates between Version 7 3-hourly TRMM Multi-
17 Satellite Precipitation Analysis (TMPA) near-real-time and research products,
18 *Atmospheric Research*, 153, 119-133,
19 <http://dx.doi.org/10.1016/j.atmosres.2014.07.032>, 2015.
- 20 Lo Conti, F., Hsu, K.-L., Noto, L. V., and Sorooshian, S.: Evaluation and comparison of satellite
21 precipitation estimates with reference to a local area in the Mediterranean Sea,
22 *Atmospheric Research*, 138, 189-204,
23 <http://dx.doi.org/10.1016/j.atmosres.2013.11.011>, 2014.
- 24 Maraun, D.: Bias Correcting Climate Change Simulations - a Critical Review, *Current Climate
25 Change Reports*, 2, 211-220, 10.1007/s40641-016-0050-x, 2016.
- 26 Marcos, R., Llasat, M. C., Quintana-Seguí, P., and Turco, M.: Use of bias correction techniques
27 to improve seasonal forecasts for reservoirs — A case-study in northwestern
28 Mediterranean, *Science of The Total Environment*, 610–611, 64-74,
29 <https://doi.org/10.1016/j.scitotenv.2017.08.010>, 2018.
- 30 Matos, J. P., Cohen Liechti, T., Juízo, D., Portela, M. M., and Schleiss, A. J.: Can satellite based
31 pattern-oriented memory improve the interpolation of sparse historical rainfall
32 records?, *Journal of Hydrology*, 492, 102-116,
33 <http://dx.doi.org/10.1016/j.jhydrol.2013.04.014>, 2013.

- 1 Meier, P., Frömelt, A., and Kinzelbach, W.: Hydrological real-time modelling in the Zambezi
2 river basin using satellite-based soil moisture and rainfall data., *Hydrol. Earth Syst.*
3 *Sci.*, 15, 999-1008, 2011.
- 4 Meyer, H., Drönner, J., and Nauss, T.: Satellite-based high-resolution mapping of rainfall over
5 southern Africa, *Atmos. Meas. Tech.*, 10, 2009-2019, 10.5194/amt-10-2009-2017,
6 2017.
- 7 Moazami, S., Golian, S., Kavianpour, M. R., and Hong, Y.: Comparison of PERSIANN and V7
8 TRMM Multi-satellite Precipitation Analysis (TMPA) products with rain gauge data
9 over Iran, *International Journal of Remote Sensing*, 34, 8156-8171,
10 10.1080/01431161.2013.833360, 2013.
- 11 Müller, M. F., and Thompson, S. E.: Bias adjustment of satellite rainfall data through stochastic
12 modeling: Methods development and application to Nepal, *Advances in Water*
13 *Resources*, 60, 121-134, <http://dx.doi.org/10.1016/j.advwatres.2013.08.004>, 2013.
- 14 Najmaddin, P. M., Whelan, M. J., and Balzter, H.: Application of Satellite-Based Precipitation
15 Estimates to Rainfall-Runoff Modelling in a Data-Scarce Semi-Arid Catchment,
16 *Climate*, 5, 32, 2017.
- 17 NIST/SEMATECH: e-handbook of statistical methods. Croarkin, C., Tobias, P., and Zey, C.
18 (Eds.), NIST ;, [Gaithersburg, Md.] ;, 2001.
- 19 Pereira Filho, A. J., Carbone, R. E., Janowiak, J. E., Arkin, P., Joyce, R., Hallak, R., and Ramos,
20 C. G. M.: Satellite Rainfall Estimates Over South America – Possible Applicability to
21 the Water Management of Large Watersheds1, *JAWRA Journal of the American Water*
22 *Resources Association*, 46, 344-360, 10.1111/j.1752-1688.2009.00406.x, 2010.
- 23 Rientjes, T. H. M., Muthuwatta, L. P., Bos, M. G., Booij, M. J., and Bhatti, H. A.: Multi-variable
24 calibration of a semi-distributed hydrological model using streamflow data and
25 satellite-based evapotranspiration, *Journal of Hydrology*, 505, 276-290,
26 <http://dx.doi.org/10.1016/j.jhydrol.2013.10.006>, 2013b.
- 27 Romano, F., Cimini, D., Nilo, S., Di Paola, F., Ricciardelli, E., Ripepi, E., and Viggiano, M.:
28 The Role of Emissivity in the Detection of Arctic Night Clouds, *Remote Sensing*, 9,
29 406, 2017.
- 30 Romilly, T. G., and Gebremichael, M.: Evaluation of satellite rainfall estimates over Ethiopian
31 river basins, *Hydrol. Earth Syst. Sci.*, 15, 1505-1514, 10.5194/hess-15-1505-2011,
32 2011.
- 33 Seo, D. J., Breidenbach, J. P., and Johnson, E. R.: Real-time estimation of mean field bias in
34 radar rainfall data, *Journal of Hydrology*, 223, 131-147,
35 [http://dx.doi.org/10.1016/S0022-1694\(99\)00106-7](http://dx.doi.org/10.1016/S0022-1694(99)00106-7), 1999.

- 1 Shrestha, M. S.: Bias-adjustment of satellite-based rainfall estimates over the central
2 Himalayas of Nepal for flood prediction. PhD thesis, Kyoto University, 2011.
- 3 Smiatek, G., Kunstmann, H., and Senatore, A.: EURO-CORDEX regional climate model
4 analysis for the Greater Alpine Region: Performance and expected future change,
5 Journal of Geophysical Research: Atmospheres, 121, 7710-7728,
6 10.1002/2015JD024727, 2016.
- 7 Srivastava, P. K., Islam, T., Gupta, M., Petropoulos, G., and Dai, Q.: WRF Dynamical
8 Downscaling and Bias Correction Schemes for NCEP Estimated Hydro-Meteorological
9 Variables, Water Resources Management, 29, 2267-2284, 10.1007/s11269-015-0940-z,
10 2015.
- 11 Switanek, M. B., Troch, P. A., Castro, C. L., Leuprecht, A., Chang, H. I., Mukherjee, R., and
12 Demaria, E. M. C.: Scaled distribution mapping: a bias correction method that preserves
13 raw climate model projected changes, Hydrol. Earth Syst. Sci., 21, 2649-2666,
14 10.5194/hess-21-2649-2017, 2017.
- 15 Taylor, K. E.: Summarizing multiple aspects of model performance in a single diagram, Journal
16 of Geophysical Research: Atmospheres, 106, 7183-7192, 10.1029/2000JD900719,
17 2001.
- 18 Tesfagiorgis, K., Mahani, S. E., Krakauer, N. Y., and Khanbilvardi, R.: Bias correction of
19 satellite rainfall estimates using a radar-gauge product – a case study in
20 Oklahoma (USA), Hydrol. Earth Syst. Sci., 15, 2631-2647, 10.5194/hess-15-2631-
21 2011, 2011.
- 22 Themeßl, M. J., Gobiet, A., and Heinrich, G.: Empirical-statistical downscaling and error
23 correction of regional climate models and its impact on the climate change signal, Clim.
24 Change, 112, 449–468 2012.
- 25 Thiemiig, V., Rojas, R., Zambrano-Bigiarini, M., Levizzani, V., and De Roo, A.: Validation of
26 Satellite-Based Precipitation Products over Sparsely Gauged African River Basins,
27 Journal of Hydrometeorology, 13, 1760-1783, 10.1175/jhm-d-12-032.1, 2012.
- 28 Thiemiig, V., Rojas, R., Zambrano-Bigiarini, M., and De Roo, A.: Hydrological evaluation of
29 satellite-based rainfall estimates over the Volta and Baro-Akobo Basin, Journal of
30 Hydrology, 499, 324-338, 10.1016/j.jhydrol.2013.07.012, 2013.
- 31 Thorne, V., Coakeley, P., Grimes, D., and Dugdale, G.: Comparison of TAMSAT and CPC
32 rainfall estimates with rain gauges, for southern Africa, International Journal of Remote
33 Sensing, 22, 1951-1974, 10.1080/01431160118816, 2001.

- 1 Tian, Y., Peters-Lidard, C. D., and Eylander, J. B.: Real-Time Bias Reduction for Satellite-
2 Based Precipitation Estimates, *Journal of Hydrometeorology*, 11, 1275-1285,
3 10.1175/2010JHM1246.1, 2010.
- 4 Tobin, K. J., and Bennett, M. E.: Adjusting Satellite Precipitation Data to Facilitate Hydrologic
5 Modeling, *Journal of Hydrometeorology*, 11, 966-978, doi:10.1175/2010JHM1206.1,
6 2010.
- 7 Toté, C., Patricio, D., Boogaard, H., van der Wijngaart, R., Tarnavsky, E., and Funk, C.:
8 Evaluation of Satellite Rainfall Estimates for Drought and Flood Monitoring in
9 Mozambique, *Remote Sensing*, 7, 1758, 2015.
- 10 Tsidu, G. M.: High-Resolution Monthly Rainfall Database for Ethiopia: Homogenization,
11 Reconstruction, and Gridding, *Journal of Climate*, 25, 8422-8443, 10.1175/JCLI-D-12-
12 00027.1, 2012.
- 13 Tumbare, M. J.: *Management of River Basins and Dams: The Zambezi River Basin*, edited by:
14 Tumbare, M. J., Taylor & Francis, 318 pp., 2000.
- 15 Tumbare, M. J.: *The Management of the Zambezi River Basin and Kariba Dam*, Bookworld
16 Publishers, Lusaka, 2005.
- 17 Valdés-Pineda, R., Demaría, E. M. C., Valdés, J. B., Wi, S., and Serrat-Capdevilla, A.: Bias
18 correction of daily satellite-based rainfall estimates for hydrologic forecasting in the
19 Upper Zambezi, Africa, *Hydrol. Earth Syst. Sci. Discuss.*, 2016, 1-28, 10.5194/hess-
20 2016-473, 2016.
- 21 Vernimmen, R. R. E., Hooijer, A., Mamenun, Aldrian, E., and van Dijk, A. I. J. M.: Evaluation
22 and bias correction of satellite rainfall data for drought monitoring in Indonesia, *Hydrol.*
23 *Earth Syst. Sci.*, 16, 133-146, 10.5194/hess-16-133-2012, 2012.
- 24 Wehbe, Y., Ghebreyesus, D., Temimi, M., Milewski, A., and Al Mandous, A.: Assessment of
25 the consistency among global precipitation products over the United Arab Emirates,
26 *Journal of Hydrology: Regional Studies*, 12, 122-135,
27 <http://dx.doi.org/10.1016/j.ejrh.2017.05.002>, 2017.
- 28 Wilks, D.: *Statistical Methods in the Atmospheric Sciences*, 2nd ed., Academic Press,
29 Burlington, Mass, 2006.
- 30 Woody, J., Lund, R., and Gebremichael, M.: Tuning Extreme NEXRAD and CMORPH
31 Precipitation Estimates, *Journal of Hydrometeorology*, 15, 1070-1077, 10.1175/jhm-d-
32 13-0146.1, 2014.
- 33 World Bank: *The Zambezi River Basin: A Multi-Sector Investment Opportunities Analysis -*
34 *Summary Report*. World Bank. © World Bank.

1 <https://openknowledge.worldbank.org/handle/10986/2958> License: Creative
 2 Commons Attribution CC BY 3.0., 2010a.

3 World Bank: The Zambezi River Basin: A Multi-Sector Investment Opportunities Analysis,
 4 Volume 2 Basin Development Scenarios, 2010b.

5 Worqlul, A. W., Maathuis, B., Adem, A. A., Demissie, S. S., Langan, S., and Steenhuis, T. S.:
 6 Comparison of rainfall estimations by TRMM 3B42, MPEM and CFSR with ground-
 7 observed data for the Lake Tana basin in Ethiopia, *Hydrol. Earth Syst. Sci.*, 18, 4871-
 8 4881, 10.5194/hess-18-4871-2014, 2014.

9 Wu, L., and Zhai, P.: Validation of daily precipitation from two high-resolution satellite
 10 precipitation datasets over the Tibetan Plateau and the regions to its east, *Acta Meteorol*
 11 *Sin*, 26, 735-745, 10.1007/s13351-012-0605-2, 2012.

12 Yang, X., Xie, X., Liu, D. L., Ji, F., and Wang, L.: Spatial Interpolation of Daily Rainfall Data
 13 for Local Climate Impact Assessment over Greater Sydney Region, *Advances in*
 14 *Meteorology*, 2015, 12, 10.1155/2015/563629, 2015.

15 Yin, Z. Y., Zhang, X., Liu, X., Colella, M., and Chen, X.: An assessment of the biases of satellite
 16 rainfall estimates over the tibetan plateau and correction methods based on topographic
 17 analysis, *Journal of Hydrometeorology*, 9, 301, 2008.

18 Yoo, C., Park, C., Yoon, J., and Kim, J.: Interpretation of mean-field bias correction of radar
 19 rain rate using the concept of linear regression, *Hydrological Processes*, 28, 5081-5092,
 20 10.1002/hyp.9972, 2014.

21 Zulkafli, Z., Buytaert, W., Onof, C., Manz, B., Tarnavsky, E., Lavado, W., and Guyot, J.-L.: A
 22 Comparative Performance Analysis of TRMM 3B42 (TMPA) Versions 6 and 7 for
 23 Hydrological Applications over Andean–Amazon River Basins, *Journal of*
 24 *Hydrometeorology*, 15, 581-592, doi:10.1175/JHM-D-13-094.1, 2014.

27 **Appendix 1:** Rain gauge stations in the Zambezi sub-basins showing x and y location, sub-basin they belong to, year of data
 28 availability, % of missing gaps, station elevation and distance from large-scale water bodies.

Station	Sub-basin	Zambezi classification	X Coord	Y Coord	Start date	End Date	% gaps (missing records)	Elevation (m)	Distance from lake (km)	MAP Gauge (mm yr ⁻¹)	MAP CMORP H (mm yr ⁻¹)
Marromeu	Zambezi	Lower Zambezi	36.95	-18.28	29/05/	31/12/	0.37	3	90	1075	1080
	Delta				2007	2013					
Caia	Zambezi	Lower Zambezi	35.38	-17.82	29/05/	31/12/	0.13	28	265	970.5	975
	Delta				2007	2013					
Nsanje	Shire	Lower Zambezi	35.27	-16.95	01/01/	31/12/	3.49	39	157	906.4	874
					2007	2013					
Makhanga	Shire	Lower Zambezi	35.15	-16.52	1998	2013	9.43	48	113	778.3	771
	Nchalo	Lower Zambezi	34.93	-16.23	01/01/	31/12/	0.60	64	96		

					1998	2013				726.3	725
					01/01/	31/12/					
Ngabu	Shire	Lower Zambezi	34.95	-16.50	1998	2010	0.74	89	123	736	752
					01/01/	31/12/					
Chikwawa	Shire	Lower Zambezi	34.78	-16.03	1998	2010	0.93	107	77	731.3	725
Tete					29/05/	31/12/					
(Chingodzi)	Tete	Lower Zambezi	33.58	-16.18	2007	2013	0.17	151	135	684.3	677
					29/05/	10/01/					
Chingodzi	Shire	Lower Zambezi	34.63	-16.00	2007	2013	11.8	280	101	737.7	735
					29/05/	12/09/					
Zumbo	Shire	Lower Zambezi	30.45	-15.62	2007	2012	0.16	345	<5	859.3	862
					11/06/	11/12/					
Mushumbi	Kariba	Middle Zambezi	30.56	-16.15	2008	2013	7.47	369	43	852.2	1028
					01/01/	30/03/					
Kanyemba	Tete	Middle Zambezi	30.42	-15.63	1998	2013	5.86	372	<5	859.3	862
	Zambezi				29/05/	10/01/					
Morrumbala	Delta	Lower Zambezi	35.58	-17.35	2007	2013	13.3	378	206	1011.7	1002
					01/01/	31/12/					
Mágoè	Tete	Middle Zambezi	31.75	-15.82	2009	2013	9.6	427	10	821.7	646
					01/01/	31/12/					
Muzarabani	Tete	Middle Zambezi	31.01	-16.39	1998	2013	1.14	430	49	821.3	887
					01/01/	30/11/					
Monkey	Shire	Lower Zambezi	34.92	-14.08	1998	2010	0.00	478	<5	988.5	1012
					01/01/	31/12/					
Mangochi	Shire	Lower Zambezi	35.25	-14.47	1998	2010	0.02	481	<5	1015	1042
					01/01/	31/12/					
Rukomechi	Kariba	Middle Zambezi	29.38	-16.13	1998	2013	6.40	530	68	803.9	800
					29/05/	10/01/					
Mutarara	Shire	Lower Zambezi	33.00	-17.38	2007	2013	11.7	548	201	888.2	859
	Luangw				01/01/	31/12/					
a		Middle Zambezi	31.93	-13.27	1998	2010	2.70	567	246	1092.5	1112
					01/01/	31/12/					
Mimosa	Shire	Lower Zambezi	35.62	-16.07	1998	2010	3.96	616	72	964.4	962
					01/01/	31/12/					
Kariba	Kariba	Middle Zambezi	28.80	-16.52	1998	2013	0.01	618	21	980.6	767
					01/01/	30/04/					
Balaka	Shire	Lower Zambezi	34.97	-14.98	1998	2010	0.78	618	24	778.2	754
					01/01/	31/12/					
Thyolo	Shire	Lower Zambezi	35.13	-16.13	1998	2010	0.11	624	86	789.6	787
					01/01/	31/12/					
Chileka	Shire	Lower Zambezi	34.97	-15.67	1998	2013	0.60	744	64	720.7	708
					01/01/	31/12/					
Fingoe	Tete	Middle Zambezi	31.88	-15.17	2009	2013	5.9	881	44	859.4	867
					01/01/	31/12/					
Muze	Tete	Zambezi	31.38	-14.95	2009	2013	8.8	888	75	879	800
					01/01/	01/01/					
Neno	Shire	Lower Zambezi	34.65	-15.40	1998	2010	9.14	903	64	810.7	813
					01/01/	31/12/					
Zámbye	Tete	Middle Zambezi	30.80	-15.11	2009	2013	9.8	950	56	870.5	1006
					01/01/	02/03/					
Mt Darwin	Tete	Middle Zambezi	31.58	-16.78	1998	2008	5.00	962	94	832.3	839
					01/01/	13/08/					
Chipata	Shire	Lower Zambezi	32.58	-13.55	1998	2003	1.11	995	179	1009.4	1028
					01/01/	31/12/					
Makoka	Shire	Lower Zambezi	35.18	-15.53	1998	2010	0.00	996	27	716.9	685
					01/01/	31/12/					
Livingstone	Kariba	Middle Zambezi	25.82	-17.82	1998	2013	0.00	996	107	761.2	765
					01/01/	31/12/					
Senanga	Barotse	Upper Zambezi	23.27	-16.10	1998	2013	8.90	1001	444	856.1	860
	Luangw				01/02/	31/12/					
a		Middle Zambezi	31.28	-14.25	1998	2013	0.40	1006	155	936.9	912
Petauke	Luangw				01/03/	31/12/					
	a	Middle Zambezi	32.57	-13.65	1998	2015	19.7	1028	179	1009.4	1028
Msekera	Lungue				01/01/	31/12/					
	Bungo	Upper Zambezi	22.70	-14.85	1998	2011	5.20	1033	582	835.8	838
					01/01/	31/12/					
Mongu	Barotse	Upper Zambezi	23.15	-15.25	1998	2013	0.51	1052	518	847.9	843

Kasungu	Shire	Lower Zambezi	33.47	-13.02	01/01/2003	31/07/2013	0.00	1063	89	793.2	783
Victoria Falls	Kariba	Middle Zambezi	25.85	-18.10	01/01/1998	31/12/2013	2.26	1065	107	740.8	742
Bolero	Luangwa	Middle Zambezi	33.78	-11.02	01/01/2003	31/05/2013	0.00	1070	38	639	577
Pandamatenga	Kariba	Middle Zambezi	25.63	-18.53	01/01/1998	31/12/2013	0.01	1071	151	709	771
Zambezi	Lungue	Middle Zambezi	25.63	-18.53	01/01/1998	31/12/2013	0.01	1071	151	709	771
Kabompo	Bungo	Upper Zambezi	23.12	-13.53	01/01/1998	31/12/2013	1.60	1075	611	982	976
Chichiri	Kabomb	Upper Zambezi	24.20	-13.60	01/01/1998	30/04/2005	0.08	1086	505	1045.9	1055
Chitedze	Shire	Lower Zambezi	35.05	-15.78	01/01/1998	31/12/2010	0.00	1136	40	717.3	744
Lundazi	Shire	Lower Zambezi	33.63	-13.97	01/01/2003	30/04/2013	0.00	1150	84	808.5	806
Guruve	Luangwa	Middle Zambezi	33.20	-12.28	01/01/2003	30/03/2013	1.40	1151	91	778.8	774
Kaoma	Tete	Middle Zambezi	30.70	-16.65	01/01/1998	31/11/2013	0.02	1159	86	866.1	870
Bvumbwe	Barotse	Upper Zambezi	24.80	-14.80	01/01/1998	01/01/2013	9.89	1162	358	950	956
Kasempa	Shire	Lower Zambezi	35.07	-15.92	01/01/1998	31/12/2011	0.00	1172	59	762.2	744
Kabwe	Kafue	Middle Zambezi	25.85	-13.53	01/01/1998	13/10/2013	9.10	1185	431	1029.4	1022
Chitipa	Luangwa	Middle Zambezi	28.47	-14.45	01/01/1998	06/01/2012	1.54	1209	230	960.6	956
Mwinilunga	Shire	Lower Zambezi	33.27	-9.70	01/01/2003	31/12/2013	0.05	1288	62	1133.5	1156
Karoi	Kabomp	Upper Zambezi	24.43	-11.75	01/01/1998	31/12/2013	4.81	1319	520	1001.3	997
Solwezi	Tete	Middle Zambezi	29.62	-16.83	01/01/1998	31/12/2004	15.08	1345	88	825.8	819
Harare (Belvedere)	Kafue	Middle Zambezi	26.38	-12.18	01/01/1998	31/03/2013	0.02	1372	356	1105.2	1105
Harare (Kutsaga)	Tete	Middle Zambezi	31.02	-17.83	01/01/1998	30/09/2013	7.80	1472	209	901.4	902
Mvurwi	Tete	Middle Zambezi	31.13	-17.92	01/01/2004	11/12/2010	0.55	1488	209	901.4	902
Dedza	Tete	Middle Zambezi	30.85	-17.03	01/01/1998	31/10/2000	0.00	1494	102	834.2	828
	Shire	Lower Zambezi	34.25	-14.32	01/01/2003	31/10/2012	0.00	1575	44	762.8	762

1

2

3 **Appendix 2:** Bias correction scheme-based Taylor Diagram performance indicators (correlation coefficients, standard
4 deviations and RMSE) of rain gauge (reference) vs CMORPH estimations (corrected and uncorrected), period 1998-2013, for
5 Lower, Middle and Upper Zambezi Basin.

Sub-basin	Rainfall estimate	RMSE (mm d ⁻¹)	Correlation Coefficient	Standard Deviation (mm d ⁻¹)
Lower Zambezi	Gauge			9.38
	R-CMORPH	9.98	0.46	8.00
	PT	10.41	0.57	8.52
	QME	9.15	0.55	6.98
	EZ	10.48	0.62	6.35
	DT	9.30	0.56	6.55
	STB	8.59	0.72	7.17
Middle	Gauge			7.94

Zambezi	R-CMORPH	8.12	0.49	7.44
	PT	7.87	0.62	6.84
	QME	7.51	0.60	6.00
	EZ	10.69	0.65	6.93
	DT	8.04	0.59	6.96
	STB	7.49	0.76	6.81
Upper Zambezi	Gauge			8.29
	R-CMORPH	7.23	0.45	6.60
	PT	7.97	0.62	7.29
	QME	8.05	0.55	7.12
	EZ	11.50	0.60	8.13
	DT	7.85	0.55	6.45
	STB	0.54	0.74	7.29

1

2